The Linnean Society of London ZOOLOGICAL Journal of the Linnean Society

Zoological Journal of the Linnean Society, 2015. With 10 figures

On the evolution and diversification of an Andean clade of reptiles: combining morphology and DNA sequences of the *palluma* group (Liolaemidae: *Phymaturus*)

FERNANDO LOBO[1]*, DIEGO A. BARRASSO[2], THOMAS HIBBARD[1] and NÉSTOR G. BASSO[2]

[1]*IBIGEO (Instituto de Bio y Geociencias del Noa), Facultad de Ciencias Naturales, Universidad Nacional de Salta y CONICET, Avenida Bolivia 5150, Salta 4400, Argentina*
[2]*Instituto de Diversidad y Evolución Austral – CONICET, Blvd. Brown 2915 (U9120ACD), Puerto Madryn, Chubut, Argentina*

Received 28 November 2014; revised 23 July 2015; accepted for publication 30 July 2015

Phymaturus comprises 44 species mainly distributed along the south-west of South America on both sides of the Andes. In this study we present a phylogenetic analysis of *Phymaturus* of the *palluma* group, one of its two large clades, including almost all described species. This analysis duplicates the number of in-group taxa compared with previous contributions. We performed a total-evidence analysis, combining molecular and morphological characters: sequencing fragments of cytochome *b* (cyt*b*), *12S*, and *ND4*, for all terminals; describing 45 new morphological characters; and incorporating all DNA sequences available from GenBank. Separate analyses of morphology and DNA partitions are presented and discussed in detail. Seven subclades are recognized here. We named three new subclades and redefined another, found to be paraphyletic. In order to recognize lineages within the traditional *Phymaturus palluma* group we proposed to treat it as a natural group, containing within it the ranks of clade, subclade, and lineages, respectively. The *palluma* group is composed by the *vociferator* and the *bibronii* clades. The *vociferator* clade, composed of Chilean and Argentinean species, would be the most basal in the group. Within the *bibronii* clade, the *roigorum* subclade includes the *Phymaturus verdugo* lineage, whereas the *mallimaccii* subclade would consist of 13 terminal taxa, for which three Chilean species have been added. In this study, morphological apomorphies are identified for all clades and the evolution of 'male head melanism' is discussed.

doi: 10.1111/zoj.12335

ADDITIONAL KEYWORDS: phylogenetic relationships – *Phymaturus* – taxonomic congruence – total evidence.

INTRODUCTION

Phymaturus is a clade of iguanian lizards that occurs at moderate to high elevations in western Argentina and the adjacent central region of Chile, as well as in various volcanic tablelands of the Patagonian region of Argentina (Lobo & Quinteros, 2005). All species are viviparous, saxicolous herbivores and are nearly always found syntopically with one or more species of *Liolaemus*, their sister clade (Etheridge & Espinoza, 2000; Schulte, Valladares & Larson, 2003; Espinoza, Wiens & Tracy, 2004). *Phymaturus* was previously divided into two groups by Etheridge (1995), with six species in the *patagonicus* group and four in the *palluma* group. In the composition of the *palluma* group, Etheridge (1995) included species known at this time: *Phymaturus palluma* (Molina, 1782), *Phymaturus mallimaccii* Cei, 1980, *Phymaturus antofagastensis* Pereyra, 1985, and *Phymaturus punae* Cei, Etheridge & Videla, 1983. Later, *Phymaturus verdugo* Cei & Videla, 2003 and *Phymaturus vociferator*

*Corresponding author. E-mail: fercholobo@gmail.com

Pincheira-Donoso, 2004 were also described as members of the *palluma* group. In a comprehensive taxonomic revision and phylogenetic study, Lobo & Quinteros (2005) described four new species of *Phymaturus*, one of which belongs to the *palluma* group: *Phymaturus dorsimaculatus* Lobo & Quinteros, 2005. However, Pincheira-Donoso, Scolaro & Sura (2008) claimed that *P. dorsimaculatus* is a synonym of *P. vociferator*, although later these taxa were found to be more closely related to other terminals than to one another by Morando *et al*. (2013), based on DNA sequences. Lobo & Abdala (2007) studied populations of southern and central Mendoza Province (Argentina), inhabiting a pair of ancient volcanic elevations located in the area called 'Payunia' by biogeographers (Roig-Juñent, Domínguez & Flores, 2006), and described *Phymaturus roigorum* Lobo & Abdala, 2007 (*palluma* group). Corbalán, Scolaro & Debandi (2009) found a population in Laguna Diamante (Mendoza) that was considered different from the other populations known in this region (*P. verdugo*, *P. palluma*, and *P. roigorum*), and described *Phymaturus gynechlomus* Corbalán, Scolaro & Debandi, 2009. In Lobo, Abdala & Valdecantos (2012a), and more recently in Lobo & Etheridge (2013), *P. gynechlomus* is considered a synonym of *P. palluma*, contrary to the assertion made by Scolaro (2010). Lobo, Abdala & Valdecantos (2010) described four new species from Argentina, including two assigned to the *palluma* group: *Phymaturus querque* Lobo *et al*., 2010 and *Phymaturus laurenti* Lobo *et al*., 2010. *Phymaturus querque* is the southernmost distributed species of the *palluma* group in Argentina, inhabiting the region of Laguna Blanca in Neuquén Province (39°08′S, 70°25′W). Recent studies made on samples of *Phymaturus* from northern Argentina resulted in the formal description of new taxa: *Phymaturus extrilidus* Lobo, Espinoza, Sanabria & Quiroga, 2012b endemic of Sierra La Invernada, San Juan Province; *Phymaturus denotatus* Lobo, Nenda & Slodki, 2012c, from Laguna Blanca of Catamarca Province; *Phymaturus aguanegra* Lobo, Laspiur & Acosta, 2013 and *Phymaturus williamsi* Lobo, Laspiur & Acosta, 2013, from the Andean massif of San Juan Province; and *Phymaturus tromen* Lobo & Nenda, 2015, from Neuquen Province. The richness of *Phymaturus* species from the Chilean side of the Andes was underestimated until recently. Núñez *et al*. (2010) described four species of the *palluma* group (*Phymaturus darwini*, *Phymaturus maulense*, *Phymaturus paihuanense*, and *Phymaturus alicahuense*), Troncoso-Palacios & Lobo (2012) described *Phymaturus damasense*, Troncoso-Palacios *et al*. (2013) resurrected *Phymaturus bibronii* (Guichenot, 1848), from the Ovalle Region (Chile), and Troncoso-Palacios & Esquerré (2014) described *Phymaturus aguedae*. An updated list of recognized species (22) of the *palluma* group is shown in Table 1. About the phylogeny and relationships of the *palluma* group, the first approach was made by Lobo & Quinteros (2005); at that time a data set of 133 characters and 22 terminal taxa was analysed, finding several results that were confirmed in later investigations (Lobo *et al*., 2012a; Morando *et al*., 2013): (1) the *palluma* species group was recovered as monophyletic, supported by several apomorphies; (2) *P. dorsimaculatus*, the population reported from Chillán (Chile) and *P. querque* were found as basal to the group; and (3) the monophyly of a clade endemic from the Puna region of Argentina was recovered. Seven years later, a new morphological analysis was performed by Lobo *et al*. (2012a). This new analysis included 206 characters and 36 terminal taxa, and gave confirmation to those previous results. In addition, a new hypothesis was proposed for the genus, revealing inner relationships within the 'Puna' clade. The main nodes found by Lobo *et al*. (2012a) were confirmed by a recent DNA analysis (Morando *et al*., 2013). In Figure 1 we show congruent nodes recovered in both independent studies. Note that even when only half of the terminal taxa are shared between Lobo *et al*. (2012a) and Morando *et al*. (2013), and different optimality criteria for building the trees were used (parsimony and Bayesian analysis), around half of the nodes remain the same. After pruning these two trees (by eliminating terminal taxa not shared by both analyses), an identical topology arises, with the exception of the position of *P. roigorum* (Fig. 1B and D). Here we report new information (molecular and morphological characters) and include all taxa belonging to the species groups (except two). The main goal of the present study is the search for a total-evidence hypothesis for the *palluma* species group, integrating molecular and morphological evidence, and the evaluation of morphological features within the group.

MATERIAL AND METHODS

Terminal taxa

In the present analysis we included 34 terminal taxa of the *palluma* group: 19 from the previous morphological study of Lobo *et al*. (2012a), ten taxa from the DNA analysis of Morando *et al*. (2013), previously not considered in the morphological analysis, and additionally five Chilean species not included in any previous analysis – *P. maulense*, *P. paihuanense*, *P. damasense*, and *P. aguedae* (Núñez *et al*., 2010; Troncoso-Palacios & Lobo, 2012; Troncoso-Palacios & Esquerré, 2014), and *P. bibronii*, recently resurrected by Troncoso-Palacios *et al*. (2013). This present analysis almost doubles the number of in-group taxa in comparison with both previous contributions recently published (19 species, Lobo *et al*., 2012a; 20 species, Morando *et al*., 2013).

Table 1. Species of the *Phymaturus palluma* group (22)

Species/authors	Terra typica
P. aguanegra Lobo, Laspiur & Acosta, 2013	Paso Agua Negra, San Juan (ARG)
P. aguedae Troncoso-Palacios & Esquerré 2014	Cerro Provincia, región Metropolitana (CHI)
P. alicahuense Núñez *et al*., 2010	Quebrada de Piuquenes, Región de Valparaíso (CHI)
P. antofagastensis Pereyra, 1985	Los Nacimientos, Catamarca (ARG)
P. bibronii (Guichenot, 1848)	Cordillera de Ovalle, Región de Coquimbo (CHI)
P. damasense Troncoso-Palacios & Lobo, 2012	Las Damas river, Termas del Flaco (CHI)
P. darwini Núñez *et al*., 2010	Valle Riecillo, Región de Valparaíso (CHI)
P. denotatus Lobo *et al*. 2012c	Laguna Blanca, Catamarca (ARG)
P. dorsimaculatus Lobo & Quinteros, 2005	Copahue, Neuquén (ARG)
P. extrilidus Lobo *et al*., 2012b	Sierra La Invernada, San Juan (ARG)
P. laurenti Lobo *et al*., 2010	Near El Peñón, Catamarca (ARG)
P. mallimaccii Cei, 1980	Sierra de Famatina, La Rioja (ARG)
P. maulense Núñez *et al*., 2010	Reserva Nacional Altos de Lircay (CHI)
P. paihuanense Núñez *et al*., 2010	Valle Los Piuquenes, Coquimbo (CHI)
P. palluma (Molina, 1782)	Cordón del Portillo, Mendoza (ARG)
P. punae Cei *et al*., 1983	Sierra de San Guillermo, San Juan (ARG)
P. querque Lobo, Abdala & Valdecantos, 2010	Laguna Blanca, Neuquén (ARG)
P. roigorum Lobo & Abdala, 2007	Nevado and Payún, Mendoza (ARG)
P. tromen Lobo & Nenda, 2015	ca. Tromen volcano, Neuquén (ARG)
P. verdugo Cei & Videla, 2003	ca. PeteroaVolcano, Mendoza (ARG)
P. vociferator Pincheira-Donoso, 2004	Laguna del Laja, Bío-Bío (CHI)
P. williamsi Lobo *et al*. 2013	40 km west of Calingasta, San Juan (ARG)

Updated species list of Lobo *et al*. (2013). Original descriptions and type locality are indicated for each case. In the present study we added 14 undescribed or/and candidate species to the cladistic analysis

Sequenced genes and the addition of GenBank information

Morando *et al*. (2013) sequenced two mitochondrial fragments [cytochrome *b* (cyt*b*) and *12S*], four protein-coding nuclear genes (*Cmos*, *NTF3*, *PLRL*, and *PNN*), and seven anonymous nuclear loci (*Phy38*, *Phy41*, *Phy60*, *Phy64*, *Phy84*, *Phy87*, and *Phy89*) of *Phymaturus*, totalling ~9100 pairs of bases. In this study we discard the *Phy87* anonymous nuclear loci because of a lack of available sequences for the *palluma* group. We added a total of 46 new DNA sequences, and nine fragments of *ND4* were merged with terminals provided by Morando *et al*. (2013): *P.* cf. *palluma* (here named *P.* sp. usp), *P. dorsimaculatus*, *P. extrilidus*, *P. laurenti*, *P. mallimacii*, *P. querque*, *P. roigorum*, *Phymaturus somuncurensis* Cei & Castro, 1973, and *P.* sp. 1 (here named *P. tromen*). The other 37 fragments correspond with ten terminals not included in previous molecular analysis, with three mitochondrial genes (cyt*b*, *ND4*, and *12S*) and one nuclear gene (*Cmos*): *P. aguedae*, *P. antofagastensis*, *P. bibronii*, *P. damasense*, *P. denotatus*, *P. gynechlomus* (= *P. palluma* from Laguna Diamante), *P. paihuanense*, *P.* sp. fia (Fiambalá, La Rioja), *P.* sp. gua (Gualcamayo, San Juan), and *P. williamsi* (see Appendix 1). Genomic DNA was extracted from tissues (liver or muscle) preserved in ethanol 96% using the phenol/chloroform method (Sambrook & Russell, 2001). The molecular markers were amplified following standard polymerase chain reaction (PCR) procedures, the primers used were G73 (5′-GCGGTAAAGCAGGTGAAGAAA-3′) and G78 (5′-AGRGTGATRWCAAANGARTARATGTC-3′), for the nuclear fragment of *Cmos* (Saint *et al*., 1998); ND4 (5′-CACCTATGACTACCAAAAGCTCATGTAGAAGC-3′) and Leu (5′-CATTACTTTTACTTGGATTTGCACCA-3′), for the *ND4* fragment (Arévalo, Davis & Sites, 1994); 12e (5′-GTRCGCTTACCWTGTTACGACT-3′) and tPhe (5′-AAAGCACRGCACTGAAGATGC-3′), for the *12S* fragment (Wiens, Reeder & Montes de Oca, 1999); and GLUDGL (5′-TGACTTGAARAACCAYCGTTG-3′) and CB3–3′ (5′-GGCAAATAGGAARTATCATTC-3′), for cyt*b* (Palumbi, 1996). Sequencing reactions were run using Big Dye Terminators 3.1 in an ABI 3130 Genetic Analyzer (Applied Biosystems). All samples were sequenced in both directions and the contigs were made using DNA BASER 3 (Heracle BioSoft, Pitesti, Romania). Sequences were edited with BioEdit (Hall, 1999), and each gene was aligned with ClustalW (Thompson, Higgins & Gibson, 1994), run in BioEdit under default parameters and subsequently concatenated with SequenceMatrix 1.7 (Vaidya, Lohman & Meier, 2011). The list of GenBank accession numbers are presented in Appendix 1.

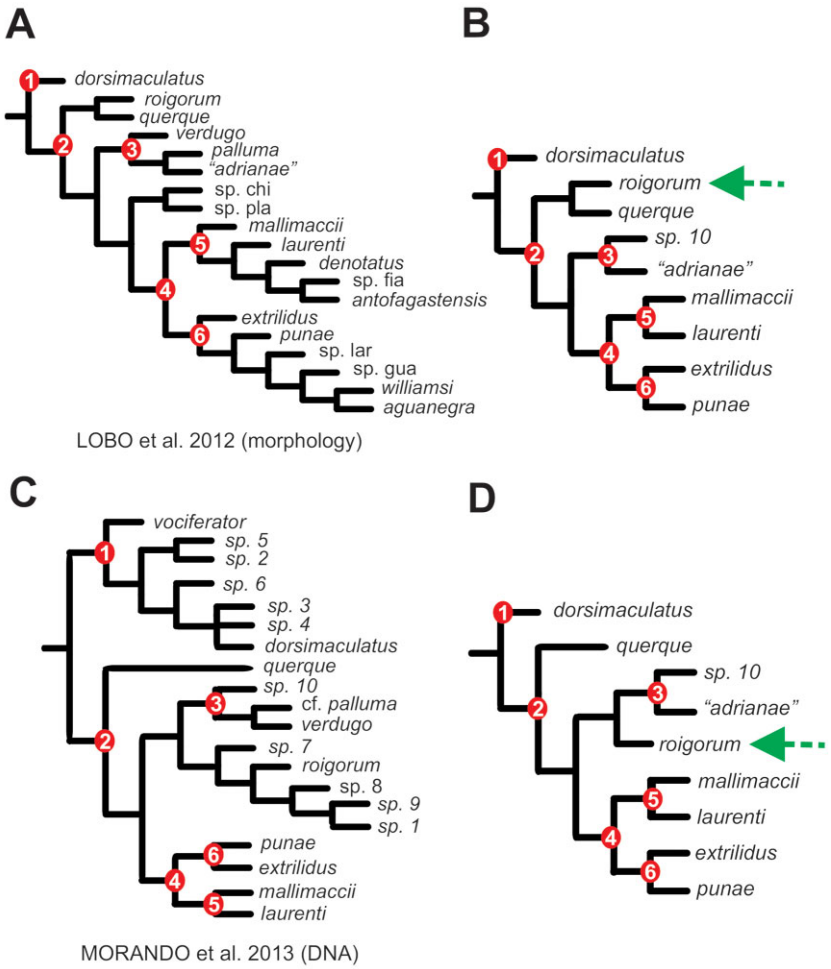

Figure 1. A, C, recent *Phymaturus palluma* group topologies published using different sources of data. A, morphological hypothesis of Lobo *et al*. (2012a); B, molecular ('all genes') topology of Morando *et al*. (2013). Numbers indicates congruent nodes (relationships) between both studies. Even though these two studies share only half of the terminal taxa, respectively, and different optimality criteria for phylogenetic analyses were used (parsimony versus Bayesian), almost half of the resulting nodes are congruent. B, D, Pruning these two topologies (deleting terminal taxa not shared by both analyses), the same topology is recovered for both studies, with the exception of the position of *Phymaturus roigorum*.

MORPHOLOGICAL CHARACTERS AND ANALYSIS

A detailed character list, including definitions, character states, and figures, is provided in Appendix 2. Data on external morphology of all terminals was obtained upon examination of 443 fluid-preserved specimens, listed in Appendix 3. The morphological data matrix includes 254 characters. In the present study, 45 new morphological characters plus two biological (presence/absence of salt excretion and fecundity as number of embryos) were revisited across the genus. Eighty per cent of this data matrix involves informative characters (205; we have kept the whole data matrix of Lobo *et al*., 2012a, built for the entire genus), because several characters exhibit informative variation only within the *patagonicus* group, and other characters are apomorphies of both clades (*patagonicus* and *palluma* groups). Eleven of these characters are informative only within the *patagonicus* group, but all are included in this study to provide the most complete and updated list. Skeletal data were obtained from 32 specimens representing 11 species of the *Phymaturus palluma* group (bone characters represent 15% of the total morphological data set). All skeletons (nine species) are wet preparations made following the standard clearing and staining techniques described in Wassersug (1976), whereas R. Etheridge skeletal collection (REE-SDSU) are dry skeletons. Skeletal data of *P. paihuanense* and *P. maulense* were taken from the original description (Núñez *et al*., 2010). This list of characters includes binary and multistate characters. Binary polymorphisms were treated as 'scaled' polymorphic species, with an intermediate state '1' in

an ordered series between species without that state (0) and species with that state (2) (Wiens, 2000). In a complementary analysis those binary polymorphic characters were scored as missing entries (?), but the same final topologies were recovered. Multistate polymorphisms were scored in each case indicating all states present for each taxon. A block of 53 continuous characters was also included in the analysis (morphometric or meristics). We selected 11 measures following Laurent (1986) and eight measures from Lobo *et al*. (2012a). Continuous characters were analysed, making ranges for each individual character for each species. TNT (Goloboff, Farris & Nixon, 2003) uses 'Farris optimization' (Farris, 1970) to estimate distances and costs among ranges: when ranges between two terminals overlap, TNT assumes zero cost. In this study we entered ranges for continuous data into the program, considering means ± SDs as ranges for any continuous character, and we standardized every continuous character by dividing the minimum and maximum value of each species by the maximum value found among species: in this way forming a new range for each species that varies between 0 and 1. Later we multiplied this range by ten. In this way the costs of transformations among states of the continuous characters were estimated as being similar to those for discrete characters.

Optimality criteria and choice of tree-building method

The total-evidence analysis (TEA) was performed applying strict parsimony in TNT (Tree Analysis using New Technology; Goloboff *et al*., 2003). We used TNT because it is the only software that allows for the analysis of continuous and discrete character blocks at the same time, with continuous characters scored as ranges. We made a 'traditional search' applying tree bisection and reconnection (TBR), with 10 000 replications (saving 20 trees per replication).

The morphology data set was analysed applying strict parsimony and the implied weights method. This method allows for weighting against homoplasy and is recommended for morphological characters because it improves clade support (Goloboff, 1993; Goloboff *et al*., 2008). Also, in a previous study (Lobo *et al*., 2012a) congruence with the molecular analysis was increased by using this method (Espinoza *et al*., 2004). The criterion of weighting against homoplasy has been previously presented by Farris (1969; 1983), and further discussion and analysis of this criterion is found in Goloboff (1995, 1997), Ramírez (2003), Aguilera & Mirande (2005), and Mirande (2009). As there is no decisive criterion to determine which values should be used for the concavity constant (k; for an alternative methodological proposal, see Mirande, 2009), Lobo *et al*., (2012a) explored a wide range of values, looking for all topologies with k = 1, 2, 3 . . . etc. to higher values (lower weighting), until finding the same topology found in a regular unweighted strict parsimony analysis. The hypothesis obtained with k = 3 (Lobo *et al*., 2012a) found a complete congruent topology with the molecular topology of Espinoza *et al*. (2004). Because of this previous finding we used k = 3 in this study for our implied-weights analysis.

The molecular partition was analysed by applying strict parsimony and Bayesian inference in order to compare our results with those of Morando *et al*. (2013). Strict parsimony was performed using TNT, applying TBR (10 000 replicates). To find the best-fitting model for the in-group we used the Akaike information criterion in jModelTest 2 (Darriba *et al*., 2012), without a partition matrix. The selected model was TrN + G + I. Bayesian analyses were conducted with BEAST 1.8 (Drummond *et al*., 2012) using the tree prior Yule process, with a randomly generated starting tree, and default values were used with the 'Auto Optimize' option. We computed 25 000 000 generations, sampled every 2500 generations, after which we examined the stationarity of parameters using TRACER 1.5: all ESS values were >200. The maximum clade credibility tree was computed with TREE ANNOTATOR 1.8, and the first 20% of the samples were discarded as burn-in. In both the parsimony molecular analysis alone and TEA, gaps were treated as a fifth state. Support for individual nodes was assessed with jackknifing resampling (Siddall, 1995) using 1000 replicates. The evolution of male head melanism was mapped using TNT (Goloboff *et al*., 2003), applying Wagner optimization (or additive optimization, i.e. Farris optimization; Wiley *et al*., 1991).

RESULTS

Cladistic analyses

Morphology and molecules combined

Total-evidence analysis comprises 9442 characters (254 morphological and 9188 nucleotide positions), and was performed applying strict parsimony; we recovered eight trees of 2 335 717 steps. The topology of the strict consensus tree is shown in Figure 2. Six of the recovered internal nodes were previously described and discussed in Lobo *et al*. (2012a) and Morando *et al*. (2013), and named as clade or group, respectively (Fig. 1). To allow easy comparisons we use the same number for the nodes as presented in Figure 1.

The clade represented by node 1 was called the *vociferator* group in Morando *et al*. (2013). The group is composed by *P. dorsimaculatus*, *P. vociferator*, *P. damasense*, *P. maulense*, and six other terminal taxa that represent potential new species (Fig. 2, node 1).

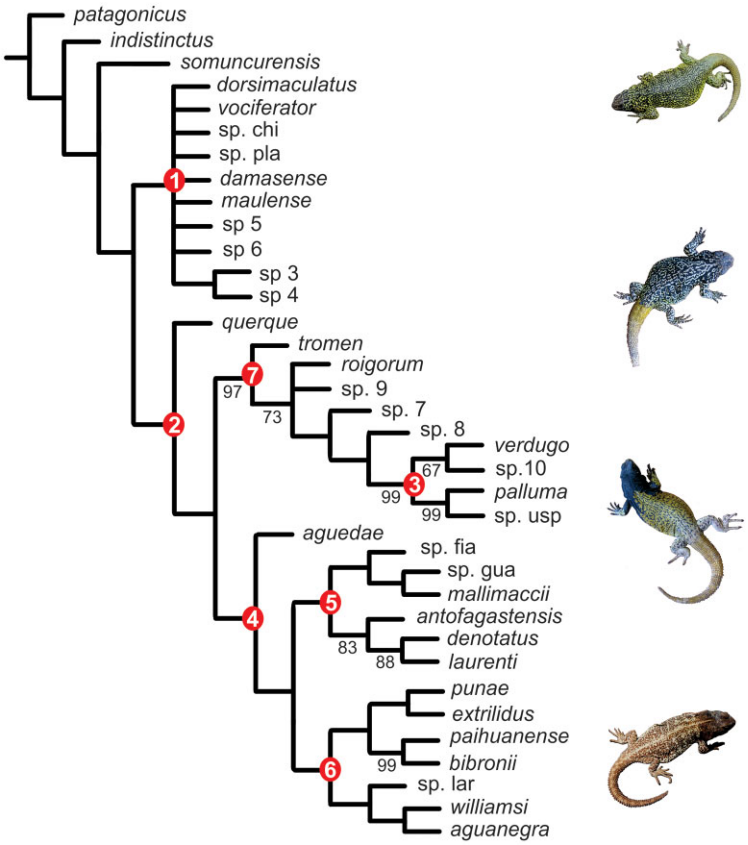

Figure 2. The total-evidence consensus tree. Red nodes, numbered 1–6, are those found in previous studies (see Fig. 1): node 1, *vociferator* clade (*vociferator* group of Morando *et al*., 2013); node 2, *bibronii* clade (present study); node 3, *verdugo* lineage (clade F of Lobo *et al*., 2012a; *verdugo* group of Morando *et al*., 2013); node 4, *mallimaccii* subclade (clade G of Lobo *et al*., 2012a; *mallimacci* group of Morando *et al*., 2013); node 5, *antofagastensis* lineage (clade H of Lobo *et al*., 2012a); node 6, *punae* lineage (clade I of Lobo *et al*., 2012a); node 7, *roigorum* subclade (*roigorum* group of Morando *et al*., 2013), but including the *verdugo* lineage (node 3). Values below branches are jackknife percentages. *Phymaturus* illustrating the tree, from top to the bottom: males of *Phymaturus damasense*, *Phymaturus roigorum*, *Phymaturus verdugo*, and *Phymaturus williamsi*. For more details, see the main text.

This group results in a politomy, possibly resulting from the lack of morphological information in four terminals (*P*. sp. 3, *P*. sp. 4, *P*. sp. 5, and *P*. sp. 6) and DNA sequences in the other two (*P*. sp. chi and *P*. sp. pla). Additionally, the examination of molecular partition matrix (9188 pb) reveals only 21 informative sites within this group. With the information considered in this study, five topologies were found in the combined analysis for the *vociferator* group. In two of them, *P. dorsimaculatus* is the basalmost species, whereas in the other tree it is *P*. sp. 6. In some cases *P. maulense* is the sister taxon of *P*. sp. 6; in others, *P. damasense* is the sister taxon of *P*. sp. 5. Only in one topology is *P. damasense* sister to *P. maulense*. *P. dorsimaculatus* never was found to be the sister taxon of *P. vociferator*.

A large clade was recovered as a sister group of the *vociferator* group (Fig. 2, node 2), including *P. querque* as the basalmost species of two subclades, one of which is formed by nine species/terminals distributed in the Mendoza and Neuquén provinces of Argentina (node 7), and with the other subclade (node 4) formed by northwestern Argentinean species (distributed in the region called 'Puna' by biogeographers) plus three other Chilean species.

The clade formed by *P. palluma*, *P. roigorum*, *P. tromen*, *P. verdugo*, and five candidate species (node 7) nest in 'clade F' in Lobo *et al*. (2012a) or in the *verdugo* group of Morando *et al*. (2013) (node 3; *P. palluma*, *P*. sp. 10, *P*. sp. usp, and *P. verdugo*). In three topologies *P*. sp. 9 is sister to *P. roigorum*, being the basalmost species, whereas in the other four topologies *P. tromen* is the basalmost species, and *P*. sp. 9 is sister to all other terminals.

The sister taxon of node 7 is the most specious lineage within the *palluma* group, 'clade G' (the 'Puna group') of Lobo *et al*. (2012a). It is formed by at least 14 ter-

minal taxa, with *P. aguedae* being the basalmost taxon, and with two recognized subclades (nodes 5 and 6) that include the former clades H and I, respectively (Lobo *et al*., 2012a), but with the addition of other taxa not considered in previous studies. A septentrional subclade (the northernmost distributed subclade of species of the *mallimaccii* clade; node 5) includes *P. antofagastensis*, *P. denotatus*, *P. laurenti*, *P. mallimacci*, *P*. sp. fia, and *P*. sp. gua, and a meridional subclade (the southernmost distributed subclade of species of the *mallimaccii* clade; node 6) includes *P. aguanegra*, *P. bibronii*, *P. extrilidus*, *P. paihuanense*, *P. punae*, *P*. sp. lar, and *P. williamsi*. In the TEA, the Chilean species are included for the first time in a phylogenetic analysis falling into two different clades: (1) *P. damasense* and *P. maulense* (sp. 2 of Morando *et al*., 2013) are nested within the *vociferator* group; and (2) whereas *P. aguedae*, *P. paihuanense*, and *P. bibronii* are nested within the other clade, named 'clade G' in Lobo *et al*. (2012a) or *mallimaccii* group in Morando *et al*. (2013).

Unifying the use of names of clades and/or groups within *Phymaturus*, and specifically within the *palluma* group

In the approach made by Etheridge (1995), two *Phymaturus* species groups were recognized (*palluma* and *patagonicus*). Later, with the inclusion of more species, the same monophyletic lineages were recovered (Lobo *et al*., 2012a), but were treated as clades (clade A, B, . . . etc). In the molecular analysis of Morando *et al*. (2013), some of these lineages were again recovered and were proposed as species groups within the *palluma* and *patagonicus* species groups (*sensu* Etheridge, 1995). In order to maintain nomenclatorial stability, we will use, wherever possible, the species groups proposed by Morando *et al*. (2013), but to avoid the logical inconsistency of naming species groups within species groups (of the same hierarchical category), we here adopt the use of clade, subclade, and lineages as categories within *Phymaturus*. By way of an indented list (being consistent with the topology of Fig. 2), we have the following arrangement.

Phymaturus palluma group (Fig. 2)

vociferator clade (node 1): *P. damasense*, *P. dorsimaculatus*, *P. maulense*, *P*. sp. 3, *P*. sp. 4, *P*. sp. 5, *P*. sp. 6, *P.* sp. chi, *P*. sp. pla, and *P. vociferator*. Males of this group exhibit throats and sides of heads melanic, females exhibit acquisition of flank colour (independently within the *mallimacci* subclade) and a loss of scale organs in tails.

bibronii clade (node 2)*: *P. querque* + (*P. roigorum* clade + *mallimaccii* subclade). Members of this group exhibit posterior enlarged supralabial scales projected ventrally (Lobo *et al*., 2012a: fig. 4D) and several changes in continuous characters, such as a higher number of precloacal pores, scales in contact to mental, contact to nasal, and tails of females becoming shorter (among others).

Phymaturus querque

roigorum subclade** (node 7): *P. roigorum*, *P*. sp. 7, *P*. sp. 8, *P*. sp. 9, *P. tromen* + *verdugo* lineage (= *verdugo* group of Morando *et al*., 2013; and 'clade F' of Lobo *et al*., 2012a). Species belonging to this subclade share unpatterned tails in males (no presence of dark- and light-coloured rings), the occurrence of the 'chocolate' colour pattern in females, and an increase in the number of infralabial scales with respect to other groups.

verdugo lineage (node 3): *P. palluma*, *P*. sp. 10, *P.* sp. usp, and *P. verdugo*. Heads completely melanic in males, females can exhibit white sides of heads, and thinner reticulate dorsal pattern.

mallimaccii subclade (node 4): *P. aguedae* + (*P. antofagastensis* lineage + *P. punae* lineage). These species are easily recognized because they exhibit a dense homogeneous 'spray' dorsal pattern (present in both sexes), brown tails in males (not yellow, as in the *vociferator* clade and *roigorum* subclade), and lateral antebrachial scales round and smooth.

Phymaturus aguedae

antofagastensis lineage (node 5): *P. antofagastensis*, *P. denotatus*, *P. laurenti*, *P. mallimaccii*, *P*. sp. fia, and *P*. sp. gua. Members of this group have females and/or juveniles with transversal lighter stripes (whitish) over their backs (lost in *P. laurenti*), flank colour in females, and higher number of dorsal head scales and lateral neck scales.

punae lineage (node 6): *P. aguanegra*, *P. bibronii*, *P. extrilidus*, *P. paihuanense*, *P. punae*, *P*. sp. lar, and *P. williamsi*. Species with almost no sexual dimorphism in dorsal pattern, lower number of subocular scales, and lower number of precloacal pores in males.

*Considered as 'node of interest' by Morando *et al*. (2013) in their study.**Redefined with respect to Morando *et al*. (2013), now including the *verdugo* lineage.

Apomorphies of major clades

The *vociferator* clade (= node 1) exhibits one morphological and 16 molecular apomorphies (common apomorphies to the eight trees): throat of males change from spotted to melanic (character 116, 1→2). In some trees there are five continuous, five discrete, and 14 molecular apomorphies: throats of females change from spotted to immaculate (character 117, 1→0); sides of head in males change from immaculate to melanic (character 124, 0→1); presence of flank colour in females (character 182, 0→1); anterior process of cricoid cartilage shape changing from T-shaped to rhomboid (character 201, 1→0); scale organs under spines of dorsal and lateral tail scales becoming lost (change from one or two scales to absent; character 244, 1→0). Continuous characters are: an increase in number of

supercilliary scales (character 9); head length/snout–vent length (SVL) ratio in males (character 19); head width/SVL ratio in females (character 22); number of pterygoid teeth (character 38); and decrease in the number of maxillary teeth (character 39).

The *bibronii* clade (= node 2) includes *P. querque*, *P. roigorum*, and *P. mallimaccii* subclades. It exhibits 31 DNA changes and eight morphological apomorphies. Two of these are discrete characters: the occurrence of a divided rostral scale (character 106, 0→1); and the acquisition of posterior enlarged supralabial scales projected ventrally (character 170, 0→2). Whereas six of these are continuous characters: increase in the number of scales in contact with interparietal scale (character 7); the position of the curved supralabial scale moved posteriorly (character 12); increase in the number of scales contacting the nasal (character 14); increase in number of scales in contact with the mental scale (character 15); decreased tail length/SVL ratio in females (character 34); and increase in the number of precloacal pores in males (character 35).

The *roigorum* subclade (= node 7), including *P. roigorum*, *P.* sp. 7, *P.* sp. 8, *P.* sp. 9, *P. tromen*, and the *P. verdugo* lineage (*P. palluma*, *P.* sp. 10, *P.* sp. usp, and *P. verdugo*), is supported by three discrete morphological characters: ringed dorsal pattern of tails in males become lost (unpatterned; character 118, 1→0); presence of flank colour in females (character 182, 0→1); and the occurrence of the 'chocolate' colour pattern in females (character 237). It is also supported by one continuous character: increase in the number of infralabial scales (character 8). In addition, other 14 DNA apomorphies support this group.

The *verdugo* lineage (= node 3), including *P. palluma*, *P.* sp. 10, *P.* sp. usp, and *P. verdugo*, is supported by seven nucleotide positions. No morphological apomorphies are recovered. This is probably linked to the fact that the basal terminal taxa of this node were recovered with unknown morphology, and therefore the optimization results are ambiguous.

The *mallimaccii* subclade (= node 4), including *P. aguedae*, and the *antofagastensis* and the *punae* lineages, exhibits 14 morphological apomorphies. There are thirteen discrete characters: throat of females changing from spotted to immaculate (character 117, 1→0); sexual dimorphism in dorsal pattern lost (character 125, 1→0); dense homogeneous 'spray' pattern present in both sexes (character 126, 0→2); females brown/grey, without thin reticulation pattern over dorsum (character 134, 1→0); loss of yellow tails in males (character 137, 1→0); loss of enlarged postcloacal scales in males (character 138, 1→0); reticulated dorsum and sides of heads in males changing to homogeneous brown/grey without pattern (character 147, 1→0), loss of female pattern formed by black vertical bars prescapular, postscapular, and repeated over flanks (character 161, 1→0); dorsal melanism of neck becoming incomplete over the mid-vertebral line (character 172, 0→1); females and/or juveniles with transversal lighter stripes (whitish) over their backs (character 180, 0→1); conspicuous nasal salt excretion (character 234, 0→1); lateral antebrachial scales become round and smooth (character 242, 12→0); and loss of enlarged external postcloacal scales in males (character 243, 1→0). There is one continuous character: increase of number of scales in contact with interparietal (character 7). There are seven DNA changes.

The *antofagastensis* lineage (= node 5) is formed by six species and is supported by nine morphological apomorphies and nine DNA changes. There are two discrete characters: acquisition of flank colour in females (character 182, 0→1); and dorsal fascia of longissimus dorsi brown pigmented and transversospinalis without pigmentation (character 216, 0→3). There are seven continuous characters: decrease in the number of dorsal head scales (character 0); decrease in the number of lateral scales on neck (character 5); supralabial 8–10 curved upwards (character 12); increase in the number of subocular scales (character 13); higher number of scales separating lorilabial row from preocular scale (character 17); increase of the head height/SVL ratio in males (character 23); and decrease of the females tibia length/SVL ratio (character 32).

The *punae* lineage (= node 6), including seven species that exhibit 11 morphological characters. There is one discrete character: occurrence of multiple sternal fenestrae (character 205, 0→1). There are ten continuous characters: supralabia 6–8 curved upwards (character 12); decrease in the number of subocular scales (character 13); lower head width/SVL ratio in females (character 22); lower interorbit distance/head length ratio in females (character 26); lower internasal distance/head length ratio in females (character 28); higher trunk length/SVL ratio in males (character 29); lower number of precloacal pores in males (character 35); higher number of tracheal rings (character 36); wider clavicle (character 46); and lower largest male/largest female ratio (character 51). There are nine DNA changes.

Using only morphological information we made additional analyses, in which all terminals with no morphological information were inactivated, i.e. candidate species *P.* sp. 3–9 of Morando *et al.* (2013). We made two analyses: applying strict parsimony (SP) and implied weighting (IW, with k = 3). Performing SP we found only one tree (tree length, L = 842.115 steps), and under the weighting scheme we found one tree of fit = 74.53939 that was only 4.565 steps longer than the first tree (L = 842.115 steps; Fig. 3A and B, respectively). With respect to the TEA, we found the following differences: the *mallimacci* subclade is not monophyletic and is divided into three lineages in the IW analysis, and into two lineages in the SP analysis. Northern Chilean

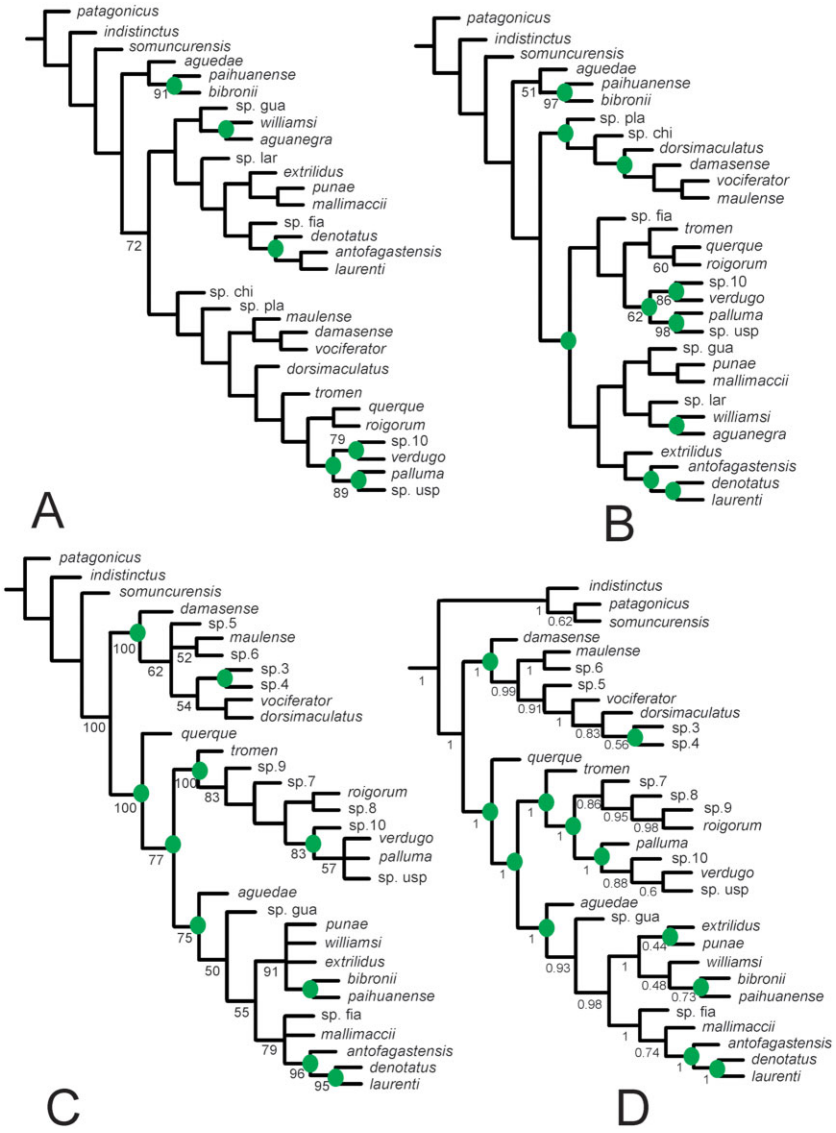

Figure 3. Independent topologies found by separate molecular and morphological analyses (the numbers below branches in A, B, and C, represent jackknife values). A, strict parsimony analysis of morphological data. B, implied weights analysis (k = 3) of morphological data. C, all-genes analysis with strict parsimony. D, Bayesian analysis of all genes concatenated. Numbers below branches represent posterior probabilities (>0.70). Green nodes are those congruent with the total-evidence analysis.

species form a natural group (*P. aguedae*, *P. bibronii*, and *P. paihuanense*), in basalmost position. In the IW analysis *P.* sp. fia is also located outside the *mallimaccii* subclade.

If these three species plus *P.* sp. fia are moved in the IW tree, a suboptimal tree of fit = 75.73889 is required to make the *mallimaccii* subclade monophyletic. If they are moved from the SP tree, a suboptimal tree (by 10 steps) is required (L = 852.088). An important set of morphological characters are unknown for *P.* sp. fia because it is a very rare animal and only females are deposited in collections, making its position unstable.

The *P. bibronii* clade is not recovered here (Fig. 3A and B). The *roigorum* subclade and *verdugo* lineage are recovered in both analyses, but including *P. querque* as a sister taxon of *P. roigorum*, whereas the *vociferator* clade is recovered in the IW analysis. As shown in Figure 3B, with TEA and IW analyses we recovered ten nodes (10/25 nodes of the tree = 40%), and in the SP analysis we recovered six nodes (6/25 nodes of the tree = 24%). As in Lobo *et al*. (2012a), morphological analysis with IW increased congruence in comparison with molecular analyses or TEA. The IW analysis recovered a topology with a less disturbed

mallimaccii subclade and a slightly better supported topology (a characteristic described by Goloboff *et al*., 2008), which was also more congruent with the TEA. In comparison with the SP analysis it is clearly an improvement. The IW analysis recovered only one or two nodes fewer than the molecular analyses.

In the morphological partition analysis the *verdugo* lineage changes its sister taxa, and in this context several apomorphies are identified. Five discrete characters were recovered: acquisition of head melanism in mature males covering sides and dorsum of head (character 124, 0→2); white lateral sides of head in females (adults or juveniles; character 144, 0→1); loss of reticulation (pattern) of dorsum and sides of heads in females becoming homogeneous brown/grey (character 146, 1→0); black vertical bars on prescapular, postscapular, and repeated over flanks absent (character 161, 1→0); and reduction in number of scale organs in temporal scales to one (character 233, 1→0). Five continuous characters were also recovered: lower number of scales contacting interparietal (character 7); higher number of scales between frontal and rostral scales (character 11); higher fragmentation of subocular scale (character 13); decrease of the head length/SVL ratio in females (character 20); and decrease of the abdominal width/SVL ratio in males (character 30).

Analysing the molecular partition alone under SP (Fig. 3C) generated six trees of $L = 1444$ steps each. Most groups found and described for the TEA are recovered: *vociferator* and *bibronii* clades, *roigorum* subclade, *verdugo* lineage, *mallimaccii* subclade, and *punae* lineage. Eleven nodes also recovered in the TEA are found (10/23 of the nodes = 43.5%). The *vociferator* clade is strongly supported and presents *P. damasense* as the basalmost taxon, sister taxon of a clade that presents a basal politomy formed by *P*. sp. 5, the pair of sister taxa *P. maulense* and *P*. sp. 6, and a terminal subclade formed by *P*. sp. 3 as sister taxon of *P*. sp. 4 and the sister taxa *P. vociferator* and *P. dorsimaculatus*. The *bibronii* clade is strongly supported, with *P. querque* as the basalmost taxon. The *roigorum* subclade is recovered with *P. tromen*, sister taxon of all other members, and *P*. sp. 9 is subsequently the basalmost taxon to a subclade formed by *P*. sp. 7 and six other terminal taxa. *Phymaturus roigorum*, sister taxon of *P*. sp. 8, is related to the *verdugo* lineage. Within the *verdugo* lineage, *P*. sp. 10 is the basalmost terminal, whereas the other three members form a politomy. The *mallimaccii* subclade presents *P. aguedae* and *P*. sp. gua as the basalmost terminal taxa. The *antofagastensis* lineage, is recovered but without the inclusion of *P*. sp. gua (the position of *P*. sp. gua in this tree as sister taxon of the two subclades *antofagastensis* and *punae* is weakly supported = 50%), and there is also a politomy among *P*. sp. fia, *P. mallimaccii*, and a very well-supported subclade formed by *P. antofagastensis*, *P. denotatus*, and *P. laurenti*. The *punae* lineage also exhibits significant support and includes a politomy formed by *P. extrilidus*, *P. punae*, *P. williamsi* and the sister taxa *P. bibronii* and *P. paihuanense*.

Under Bayesian analysis (Fig. 3D) we recovered *vociferator* and *bibronii* clades, the *roigorum* subclade, the *verdugo* lineage, the *mallimaccii* subclade, and the *punae* lineage (*antofagastensis* lineage not recovered; 12/28 of the nodes = 42.8%). The *vociferator* clade is also strongly supported and presents *P. damasense* as the basalmost taxon, sister taxon of a clade that presents the sister taxa *P. maulense* and *P*. sp. 6, related to a subclade formed by five terminal taxa, their relationships from the most basal to the most terminal being as follows: *P. dorsimaculatus*, *P*. sp. 5, *P. vociferator*, and the sister taxa *P*. sp. 3 and *P*. sp. 4. The *bibronii* clade is strongly supported, with *P. querque* as the basalmost taxon. The *roigorum* subclade is recovered with *P. tromen* as sister taxon of a couple of subclades, one of them formed by *P*. sp. 7, *P*. sp. 8, and the sister taxa *P*. sp. 9 and *P. roigorum*, and the other conforming to the *verdugo* lineage. Within the *verdugo* lineage, *P. palluma* is the sister taxon of the remaining species. *P*. sp. 10 is closely related to the pair formed by *P. verdugo* and *P.* sp. usp. The *mallimaccii* subclade presents the same basal structure of that recovered in the SP analysis, with *P. aguedae* and *P*. sp. gua recovered as the basalmost taxa of the group. The *antofagastensis* and *punae* lineages are better resolved. In *antofagastensis*, one of the original trees of the parsimony analysis exhibits the same pattern of relationships, but in the *punae* subclade two significant incongruences exist: *P. extrilidus* as sister taxon of *P. punae*, and *P. williamsi* as sister taxon of the pair *P. bibronii* and *P. paihuanense*, but both cases are weakly supported (posterior probability, PP 0.44 and 0.48).

Congruences and incongruences among different analyses

Between both morphological analyses there exist a 40% of shared nodes (60% of incongruence). As the IW analysis of morphology recovers a significantly more congruent topology with the TEA, this demonstrates that this weighting method improves morphological analyses not just in terms of reaching better statistical support (Goloboff *et al*., 2008) but also in reaching more accurate results.

Incongruence between the two molecular analyses is somewhat lower: there are 69.5% of nodes in the SP analysis that are also recovered in the Bayesian hypothesis (30.5% of incongruence between them). When we revisit the six original topologies of the parsimony analysis of the DNA partition mentioned above we find one tree more congruent with the Bayesian tree, one that recovers the same position of *P*. sp. fia within

the *antofagastensis* lineage, and one that recovers the same position of *P*. sp. 5 within the *vociferator* clade, thereby restricting the incongruence level between both analyses to 20%. Incongruences between both molecular hypotheses imply the impossibility of certain relationships found in one analysis with respect to the other. Relationships that are only recovered in the Bayesian analysis include: *Phymaturus roigorum* as sister taxon of *P*. sp. 8; *P. dorsimaculatus* as sister taxon of *P. vociferator* (only in the parsimony analysis) and the pair *P. extrilidus* and *P. punae*; *P. palluma* as the basal species of the *verdugo* lineage; and *P. williamsi* as sister taxon of *P. bibronii* and *P. paihuanense*.

Major incongruences between partitions (morphology and DNA sequences) are demonstrated by the splitting of the monophyly of the *mallimaccii* clade by the morphology analysis, where a subclade formed by *P. aguedae*, *P. bibronii*, and *P. paihuanense* is recovered as monophyletic and basal to the whole *palluma* group (but this hypothesis is not well supported in the IW analysis). *Phymaturus querque* is recovered in the morphological analysis as a sister taxon of *P. roigorum* with jackknife support of 60%. The position of *P. mallimaccii* and *P. extrilidus* is also exchanged between the *antofagastensis* and *punae* lineages in the morphological analysis, but no support is found for this hypothesis.

Evolution and ontogeny of head melanism

Melanistic heads are quite common in males of the *palluma* group (Fig. 4). All females of *P. verdugo* exhibit melanic throats and several *P. palluma* also have dark throats. The complete melanic heads of males appeared in the ancestor of the *verdugo* lineage (Fig. 5). In *P. palluma* and *P.* sp. usp the melanism in the dorsum of heads is attenuated in males, becoming almost light brown to grey in some cases (Lobo & Abdala, 2007: fig. 2C; Lobo *et al*., 2012a: character 159, 'dirty heads'). In basal taxa of the *palluma* group males show melanism only on the throats and sides of heads, as seen in species of the *vociferator* clade. Even in females of *P. dorsimaculatus* the throats are melanic (Fig. 5). In females of the *mallimacci* subclade, throat coloration is variable. Throats can be obscure in males (i.e. *P. williamsi* and *P. aguanegra*) or can be lighter, without traces of dark pigmentation (i.e. *P. denotatus* and *P. laurenti*), with the same coloration as their bellies. In northern Chilean species *P. aguedae*, *P. paihuanense*, and *P. bibronii*, no melanism is present in males and females (even in their throats; Fig. 4G). According to our phylogenetic hypothesis (Fig. 5) this dark coloration occurred in the closest ancestor of *antofagastensis* and *punae* lineages (independent of its origin in the ancestor of the *verdugo* lineage), and was a secondary loss in the pair *P. bibronii* and *P. paihuanense*. The hypotheses derived from morphology alone (Fig. 3A and B) recover a monophyletic group formed by *P. aguedae*, *P. paihuanense*, and *P. bibronii*. In this case, the lack of throat melanism and head melanism in general can be considered as apomorphies of this group. Full melanic heads arose later in the evolution of the group, as a novelty that occurred twice, independently: once in the *verdugo* lineage and once within the *mallimacci* subclade (Fig. 5). Observations made in an ontogenetic series from small juveniles to adults helped us to understand how black coloration progressively invades the throat surfaces (Fig. 4A, B and C) and sides of the head. The same pattern of development was corroborated in young specimens of *P. palluma*, but in this species melanism goes beyond covering the sides and dorsum of head. Considering that a full melanic head develops later in the ontogenetic sequence after beginning on throats, and that its origin in the phylogeny of *Phymaturus* also occurred later, this character can be explained as a terminal addition during ontogeny.

DISCUSSION

The relationships within the *palluma* group

A significant degree of congruence exists between morphological and molecular analyses (Lobo *et al*., 2012a; Morando *et al*., 2013), even when different tree-building criteria were implemented (parsimony and Bayesian analysis). The morphological hypothesis most congruent with the all-genes molecular hypothesis is the K3 topology (Fig. 1). Both *patagonicus* and *palluma* groups are recovered.

In the present study, the SP analysis of total evidence recovers the deep phylogenetic structure of the group that is fully congruent with Morando *et al*. (2013: nodes 2, 3, and 4), where the *vociferator* clade is placed as the basal group. Even when the taxon sampling in Lobo & Quinteros (2005) and Lobo *et al*., (2012a) analyses for the *vociferator* clade was very limited, *P. dorsimaculatus* (a member of this group) is always the basalmost species, the same relative position of the *vociferator* group in the molecular analysis of Morando *et al*. (2013) and TEA of this study. The Lobo & Quinteros (2005) and Lobo *et al*. (2012a) analyses differ with those of Morando *et al*. (2013) and our TEA in the fact that *P. dorsimaculatus* did not form a natural group with *P.* sp. chi + *P.* sp. pla (Lobo *et al*., 2012a: sp. 2 and sp. 3; see Figure 9). In all alternative hypotheses of Lobo *et al*. (2012a: fig. 11), *P*. sp. chi and *P*. sp. pla were placed near to *dorsimaculatus*, but were not recovered as a natural group. These three terminals along with others were recovered as a monophyletic clade both in the TEA and in the morphological analysis, i.e. the *vociferator* clade, supported by several morphological apomorphies. Note that the new matrix used

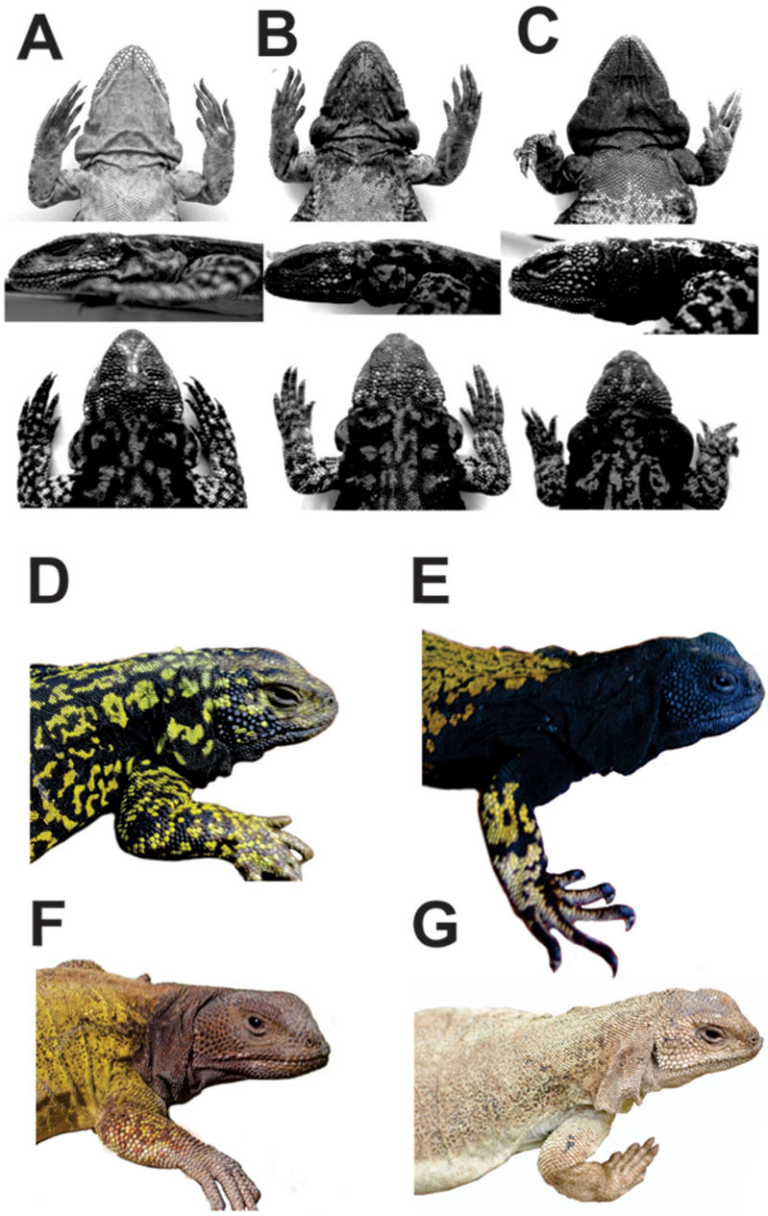

Figure 4. Ontogeny of melanism in throat, chest, sides, and dorsum of head in *Phymaturus dorsimaculatus*. A, ventral, lateral, and dorsal views of juvenile male (65.1 mm snout–vent length, SVL; MCN 1578); B, juvenile male (80.3 mm SVL; MCN 1570); C, adult male (89.8 mm SVL; MCN 1572). D–G, colour pictures of different species of males of *Phymaturus*: D, colour picture of a live *Phymaturus dorsimaculatus* male (photo by F. Lobo); E, *Phymaturus verdugo* (photo by F. Lobo); F, *Phymaturus punae* (photo by J.C. Acosta); G, *Phymaturus bibronii* (photo by A. Laspiur).

in this study has larger taxon sampling (three new terminals were added), and 45 new morphological characters.

Phymaturus roigorum and *P. querque* were obtained as sister taxa in all topologies of Lobo *et al*. (2012a) and also in our parsimony analysis with the morphological data set only. In the TEA, the two molecular analyses of this study, and the trees shown by Morando *et al*. (2013) these species are never sister species. In our analysis species belonging to the *roigorum* group of Morando *et al*. (2013) are basal to the *verdugo* linage, but do not form a monophyletic group by themselves. Only our IW morphological analysis is congruent with the nuclear and all-genes Bayesian analyses of Morando *et al*. (2013). In the mitochondrial genes analysis of Morando *et al*. (2013), their *roigorum* subclade is paraphyletic. Considering our total-evidence results, we propose redefining their *roigorum*

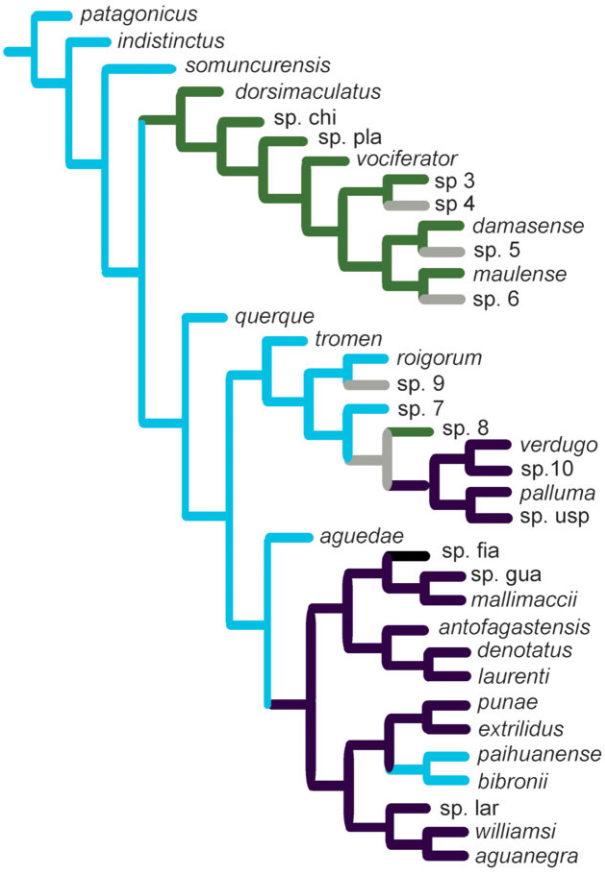

Figure 5. Evolution of head melanism, optimized on one of the eight most parsimonious trees found from total-evidence analysis for the *palluma* group (all topologies imply the same scheme of changes for this particular character); blue, melanic head pigmentation absent, reticulated pattern conspicuous or in some cases any pattern at all; green, melanic throats and sides of heads, dorsum of head reticulated; purple, complete melanic heads (throats, sides, and dorsum of heads).

group, now *roigorum* subclade, to include the *verdugo* lineage (Fig. 2). The most terminal group within the *palluma* group is 'clade G' (Lobo & Quinteros, 2005; Lobo *et al*., 2012a), called the *mallimaccii* group by Morando *et al*. (2013). This large clade is composed of two subclades, congruent in part with Lobo *et al*. (2012a). 'Clade H' (now the *antofagastensis* lineage) is fully recovered (*P. antofagastensis*, *P. denotatus*, *P.* laurenti, *P. mallimaccii*, and *P*. sp. fia), but also includes *P*. sp. gua. 'Clade I' (now the *punae* lineage) is recovered, but lacks *P*. sp. gua. The composition of 'clade G' (*mallimaccii* subclade) as recovered from the TEA is not recovered identically in both independent runs (molecular and morphological analyses). It is recovered as monophyletic in the two DNA analyses, but in both morphological analyses parts of its members are recovered as basal to the whole *palluma* group (Fig. 3A and B: *P. aguedae*, *P. bibronii*, and *P. paihuanense*).

With the inclusion of candidate species, such as those proposed by Morando *et al*. (2013), the optimization of several morphological characters that were previously found as apomorphies in Lobo *et al*. (2012a) becomes ambiguous. The morphologies of the candidate species remain unknown, so it is not possible at this time to provide more morphological apomorphies to node 7 (*roigorum* subclade; Fig. 2).

A useful methodological observation about morphological analyses can be performed after our research. Using implied weights allowed us to recover a hypothesis that is more congruent with the TEA or the molecular analyses than the un-weighted analysis. We conclude that the use of implied weights in morphological analysis not only results in better-supported clades than are produced by current unweighted analyses, as presented by Goloboff *et al*. (2008), but also results in recovering more accurate topologies.

Chilean species of *Phymaturus*

Based on our morphological data set, we found two competing topologies (Fig. 3) in the SP analysis. We found that *P. damasense*, *P. dorsimaculatus*, *P. maulense*, *P*. sp. chi, *P*. sp. pla, *P. vociferator*, and *P. vociferator* do not form a monophyletic group, but are related basally to the *roigorum* clade. Applying implied weights we recovered the *vociferator* clade as monophyletic and basal to the rest of the *palluma* group members (with the exception of three species). In the TEA, the *vociferator* clade is recovered but internal relationships are unresolved (Fig. 2). This lack of resolution can probably be explained by the absence of morphological information for half of its members, and also because of the very few informative nucleotide sites found for this group (21 of 9188). The other three nominal Chilean species of *Phymaturus* incorporated in the present study exhibit apomorphies that include them within the *mallimaccii* subclade ('Puna clade'), with the dense 'spray' pattern present in both sexes being the most conspicuous pattern present in both sexes (character 126, 0→2; Lobo & Quinteros, 2005). *Phymaturus bibronii* and *P. paihuanense* (Núñez *et al*., 2010) don't exhibit morphological divergence. Recently Troncoso-Palacios *et al*. (2013) resurrected *P. bibronii* (considered a synonym of *P. palluma* for more than a century), and they considered *P. bibronii* and *P. paihuanense* as conspecific. In all the analyses of the present study these species are recovered together; therefore, we consider these terminals as conspecific. Analysing the morphological data set it can be seen that the three species *P. aguedae*, *P. bibronii*, and *P. paihuanense* form a monophyletic group (Fig. 3A and B), but this grouping has no support and exhibits only

four apomorphies that also present changes in other sections of the tree, three of which are: nasal salt excretion; the occurrence of whitish thin strips over the back of females or juveniles; and a decrease in the number of gular scales, which also changes within the *mallimaccii* subclade (the clade that includes these taxa in the TEA).

Populations named here as *P*. sp. pla and *P*. sp. chi (El Planchón and Chillán) were considered as independent taxa, as in previous studies. In future studies we envisage that these will be proven as valid species. Although we were able to analyse scarce morphological information, it is clear that much more investigation is needed for these two taxa. There exists the possibility that *P*. sp. pla represents a population of *P. maulense*, but more information is necessary to take a definitive decision. *Phymaturus alicahuense* and *P. darwini* were not available for this study.

Biogeographic considerations

Historical biogeography based on explicit methods of analyses reported two potential ancestral areas for the genus *Phymaturus* (Díaz Gómez, 2008). Using Fitch's optimization method central Patagonia was recovered as the ancestral area of the genus, whereas DIVA analysis suggested Cordillera Andina and Valle Central as the ancestral area. The cladogram of *Phymaturus* produced by Lobo *et al*. (2012a: fig. 13) over the entire range of distribution suggested a central Patagonian origin, with subsequent radiations of both groups of genera (*palluma* and *patagonicus*) towards northern latitudes, in agreement with a hypothesis outlined by Díaz Gómez (2008). Lobo *et al*. (2012a: fig. 13) hypothesized the northernmost species within the *palluma* group (*mallimaccii* subclade), occupying areas of the Argentine Puna, splitting into a northern radiation, the *antofagastensis* lineage, and a southern radiation, the *punae* lineage. Only one species belonging to the *mallimaccii* subclade is not present in the Puna region, *P. aguedae* (Cordillera Andina), and it is the basalmost member. Relationships that are incongruent with the present analysis were the position of terminals named in Lobo *et al*. (2012a) as *P*. sp. 2 and *P*. sp 3, here named *P*. sp. chi and *P*. sp. pla, which are members of the *vociferator* clade, together with *P. dorsimaculatus*. Phylogeographic breaks, refugia, and stable areas for Patagonia were proposed recently by studying the phylogeographic patterns and distributions of *Liolaemus* lizards and plants (Sérsic *et al*., 2011). Results of this contribution would explain most of the *patagonicus* group diversification, but this analysis reaches the extreme south of the *palluma* group distribution only, making it impossible to compare with the present study. Within this *palluma* group, the greater part of the distribution of clades recognized in our study match the endemism areas described by biogeographers (Roig-Juñent *et al*., 2006): the *vociferator* clade is the most basal, and is composed of Chilean and Argentinean species. It is distributed in Cordillera Andina and Valle Central (Díaz Gómez, 2008), and in Argentina it is restricted to the western Neuquén Province, close to the Andes (*P. dorsimaculatus*, *P*. sp. 3, *P*. sp. 4, *P*. sp. 5, and *P*. sp. 6). The *roigorum* subclade is primarily distributed in the region called Payunia, composed of species living in Auca Mahuida (*P*. sp. 7 in the present analysis), near Tromen Volcano (*P. tromen*), Domuyo Volcano (*P*. sp. 8) in Neuquén Province, and Payún Volcano and Nevado Mountain (*P. roigorum*) in Mendoza Province. Northern species of the *roigorum* subclade, forming the *verdugo* lineage, are distributed along the western slopes of the Andes in Mendoza Province (*P. verdugo* and *P. palluma*), and reach the Sierra de Uspallata (*P*. sp. usp, 'Puna Cuyana') of Mendoza Province. The phylogenetic position of *P. querque* is interesting to note, as the morphological analysis includes this species in the *roigorum* subclade and it is distributed in the southern extreme of Payunia, like most other members of this group, but the TEA and molecular analyses place this species as the most basal within the *bibronii* clade. Morando *et al*. (2013) related the origin of the genus to the uplift of the Andes (~ 22 Mya) following Fontanella *et al*. (2012), contrary to that study we prefer to be more cautious about this estimation, because evolutionary rates were calibrated based on a fossil of *Liolaemus* with uncertain position in a huge clade (subgenus *Eulaemus*; Abdala & Quinteros, 2014) of more than 140 spp. According to our results and those of Morando *et al*. (2013), the molecular rates of change within *Phymaturus* seem to differ from those of its sister genus *Liolaemus*. Average genetic distances for cyt*b* between sister taxa in *Phymaturus* are calculated at around half the distances estimated for sister taxa in *Liolaemus* (Martínez, 2012). Future molecular clocks with multiple points of calibration and with a more precise phylogenetic position of fossils would be valuable in answering whether: (1) a significant degree of variation exists among rates of genetic change in different lineages of Liolaemid lizards; or (2) the diversification of *Phymaturus* is more recent than that of *Liolaemus*.

Perspectives and the need of further studies

Several pending questions about the phylogenetic relationships and taxonomy of this group remain, and new information is required regarding: the controversial position of *P*. sp. gua (a floating taxon); the incongruence between molecular and morphological analyses in the relationships of *P. querque*; the lack of DNA information for *P. aguanegra* and *P*. sp. lar; the lack of information on several morphological

characters; and the whole male morphology of *P*. sp. fia, as well as the need to revisit *P*. sp. pla and *P*. sp. chi, and the described species *P. alicahuense* and *P. darwini* (for which no sequences are available). Other taxonomic studies should attend the resolution of the taxonomic status of the Uspallata lizard, named *P.* sp. usp in this study (see specific taxonomic considerations about this lizard in Lobo & Etheridge, 2013). The careful morphological revision of the candidate species described by Morando *et al*. (2013) is also needed. With more information to hand, it will be important to define whether they can be considered full species. Finally, all 'sp.' included in the present study that clearly represent independent lineages must be formally described; *P*. sp fia, *P*. sp. gua, and *P*. sp. lar should be prioritized. At present, studies tackling most of these challenges are in progress in our lab.

ACKNOWLEDGEMENTS

We thank the anonymous referees for very useful suggestions. We thank S. Nenda, S. Valdecantos, A. Laspiur, J. Grosso, L. Cotichelli, J.C. Acosta, S. Quinteros, and C. Abdala for helping us in the field or with lab work. We thank J. Troncoso-Palacios for his important comments on a draft version of the article. This study was supported by grants (FL) from CONICET Consejo Nacional de Investigaciones Científicas y Técnicas of Argentina (PIP 2841) and CIUNSA Consejo de Investigaciones de la Universidad Nacional de Salta, Argentina (CIUNSA 2036). We thank the following colleages (and museums) for allowing F.L. to study specimens under their care over the last decade: E. Pereyra (Instituto de Biologia Animal, Universidad Nacional de Cuyo, Mendoza), F. Videla (IADIZA, Mendoza), E. Lavilla and S. Kretzschmar (Instituto de Herpetología, Fundación Miguel Lillo, Tucumán), J. Faivovich (Museo Argentino de Ciencias Naturales, Buenos Aires), H. Núñez (Museo Nacional de Historia Natural, Santiago), A. Scolaro (CENPAT, Pto. Madryn), R. Etheridge and T. Reeder (San Diego State University), J. Hanken and J. Rosado (Museum of Comparative Zoology, Harvard), J. Wiens (Carnegie Museum of Natural History, Pittsburgh), and J. McGuire (Museum of Vertebrate Zoology, Berkeley).

REFERENCES

Abdala CS, Acosta JL, Acosta JC, Alvarez BB, Arias F, Avila LJ, Blanco GM, Bonino M, Boretto JM, Brancatelli G, Breitman MF, Cabrera MR, Cairo S, Corbalán V, Hernando A, Ibargüengoytía N, Kakoliris F, Laspiur A, Montero R, Morando M, Pelegrin N, Pérez CHF, Quinteros AS, Semhan RV, Tedesco ME, Vega L, Zalba SM. 2012. Categorización del estado de conservación de las lagartijas y anfisbenas de la República Argentina. *Cuadernos de Herpetología* **26:** 215–247.

Abdala CS, Quinteros AS. 2014. Los últimos 30 años de la familia de lagartijas más diversa de Argentina. Actualización taxonómica y sistemática de Liolaemidae. *Cuadernos de Herpetología* **28:** 55–82.

Aguilera G, Mirande JM. 2005. A new species of *Jenynsia* (Cyprinodontiformes: Anablepidae) from northwestern Argentina and its phylogenetic relationships. *Zootaxa* **1096:** 29–39.

Arévalo E, Davis S, Sites JW Jr. 1994. Mitochondrial DNA sequence divergence and phylogenetic relationships among eight chromosome races of the *Sceloporus grammicus* complex (Phrynosomatidae) in central Mexico. *Systematic Biology* **43:** 387–418.

Cei JM. 1980. New iguanid lizards from the Famatina mountains of western Argentina. *Journal of Herpetology* **14:** 57–64.

Cei JM, Etheridge R, Videla F. 1983. Especies nuevas de iguánidos del noroeste de la provincia de San Juan (Reserva Provincial San Guillermo), Argentina. *Deserta* **7:** 316–323.

Cei JM, Videla F. 2003. A new *Phymaturus* species from volcanic cordilleran mountains of the south–western Mendoza province, Argentina (Liolaemidae, Iguania, Lacertilia, Reptilia). *Bolletino del Museo Regionale di Scienze Naturali (Torino)* **20:** 291–314.

Corbalán V, Scolaro JA, Debandi G. 2009. A new species of the genus *Phymaturus* of the *flagellifer* group from Central – Western Mendoza, Argentina (Reptilia: Iguania: Liolaemidae). *Zootaxa* **2021:** 42–56.

Darriba D, Taboada GL, Doallo R, Posada D. 2012. jModelTest 2: more models, new heuristics and parallel computing. *Nature Methods* **9:** 772. doi: 10.1038/nmeth.2109

Díaz Gómez JM. 2008. Historical biogeography of *Phymaturus* (Iguania: Liolaemidae) from Andean and patagonian South America. *Zoologica Scripta* **37:** 1–7.

Drummond AJ, Suchard MA, Xie D, Rambaut A. 2012. Bayesian phylogenetics with BEAUti and the BEAST 1.7. *Molecular Biology and Evolution* **29:** 1969–1973.

Espinoza RE, Wiens JJ, Tracy CR. 2004. Recurrent evolution of herbivory in small, cold–climate lizards: breaking the ecophysiological rules of reptilian herbivory. *Proceedings of the National Academy of Sciences* **101:** 16819–16824.

Etheridge RE. 1995. Redescription of *Ctenoblepharys adspersa* Tschudi, 1845, and the taxonomy of Liolaeminae (Reptilia: Squamata: Tropiduridae). *American Museum Novitates* **3142:** 1–34.

Etheridge R, Espinoza RE. 2000. Taxonomy of the Liolaeminae (Squamata: Iguania: Tropiduridae) and a semi-annotated bibliography. *Smithsonian Herpetological Information Service* **126:** 1–164.

Farris JS. 1969. A successive approximations approach to character weighting. *Systematic Zoology* **18:** 374–385.

Farris JS. 1970. Methods for computing Wagner trees. *Systematic Zoology* **19:** 83–92.

Farris JS. 1983. The logical basis of phylogenetic analysis. In: Platnick NI, Funk VA, eds. *Advances in Cladistics II*. New York: Columbia University Press, 7–36.

Fontanella F, Olave M, Avila LJ, Sites JW Jr, Morando M. 2012. Molecular dating and diversification of the South American lizard sub-genus *Eulaemus*based on nuclear and mitochondrial DNA sequences. *Zoological Journal of the Linnean Society* **164:** 825–835.

Goloboff P, Farris J, Nixon K. 2003. T.N.T.: Tree Analysis Using New Technology. Program and documentation, Available at: www.zlillo.org.ar/phylogeny

Goloboff PA. 1993. Estimating character weights during tree search. *Cladistics: The International Journal of the Willi Hennig Society* **9:** 83–91.

Goloboff PA. 1995. Parsimony and weighting: a reply to Turner and Zandee. *Cladistics: The International Journal of the Willi Hennig Society* **11:** 91–114.

Goloboff PA. 1997. Self–weighted optimization: tree searches and character state reconstructions under implied transformation costs. *Cladistics: The International Journal of the Willi Hennig Society* **13:** 225–245.

Goloboff PA, Carpenter JM, Arias JS, Miranda Esquivel DR. 2008. Weighting against homoplasy improves phylogenetic analysis of morphological data sets. *Cladistics: The International Journal of the Willi Hennig Society* **24:** 758–773.

Guichenot A. 1848. Reptilianos. In: Gay C, ed. *Historia física y política de chile*. Paris: Maulde and Renou, 1–372.

Hall TA. 1999. BioEdit: a user–friendly biological sequence alignment editor and analysis program for Windows 95/98/NT. *Nucleic Acids Symposium Series* **41:** 95–98.

Laurent RF. 1986. Descripciones de nuevos Iguanidae del género *Liolaemus*. *Acta Zoologica Lilloana* **38:** 87–105.

Lobo F, Abdala CS. 2007. Descripción de una nueva especie de *Phymaturus* del grupo de *P. palluma* de la provincia de Mendoza, Argentina. *Cuadernos de Herpetología* **21:** 103–113.

Lobo F, Abdala CS, Valdecantos S. 2010. Taxonomic studies of the genus *Phymaturus* (Iguania: Liolaemidae): description of four new species. *South American Journal of Herpetology* **5:** 102–126.

Lobo F, Abdala CS, Valdecantos S. 2012a. Morphological diversity and phylogenetic relationships within a South – American clade of iguanian lizards (Liolaemidae: *Phymaturus*). *Zootaxa* **3315:** 1–41.

Lobo F, Espinoza RE, Sanabria E, Quiroga L. 2012b. A New *Phymaturus* (Iguania: Liolaemidae) from the southern extreme of the argentine puna. *Copeia* **2012:** 12–22.

Lobo F, Etheridge R. 2013. The Type Locality of *Phymaturus palluma* (Molina, 1782) (Reptilia: Iguania: Liolaemidae) and the Status of *Phymaturus adrianae* Pereyra, 1992 and other Unnamed Populations. *South American Journal of Herpetology* **8:** 1–13.

Lobo F, Laspiur A, Acosta JC. 2013. Description of new andean species of the genus *Phymaturus* (Iguania: Liolaemidae) from Northwestern Argentina. *Zootaxa* **3683:** 117–132.

Lobo F, Nenda SJ. 2015. Discovery of two new species of *Phymaturus* (Iguania: Liolaemidae) from Patagonia, Argentina, and occurrence of melanism in the *patagonicus* group. *Cuadernos de Herpetología* **29:** 5–25.

Lobo F, Nenda SJ, Slodki D. 2012c. A new lizard of *Phymaturus* (Iguania: Liolaemidae) from Argentina. *Herpetologica* **68:** 121–133.

Lobo F, Quinteros S. 2005. A morphological approach on the phylogenetic relationships within the genus *Phymaturus* (Iguania: Liolaemidae). The description of four new species from Argentina. *Papéis Avulsos Zoologia* **45:** 143–177.

Martínez LE. 2012. Métodos empíricos para delimitar especies: el complejo Liolaemus bibronii (Squamata: Liolaemini) como ejemplo. PhD.Dissertation, Universidad Nacional de Córdoba, Córdoba, Argentina. 299 pp.

Mirande JM. 2009. Weighted parsimony phylogeny of the family Characidae (Teleostei: Characiformes). *Cladistics* **25:** 574–613.

Molina GI. 1782. *Saggio sulla storia naturale del chile*. Bologne, Italia: Stamperia di S. Tommaso d'Aquino.

Morando M, Avila LJ, Pérez CH, Hawkins MA, Sites JW Jr. 2013. A molecular phylogeny of the lizard genus *Phymaturus* (Squamata, Liolaemini): Implications for species diversity and historical biogeography of southern South America. *Molecular Phylogenetics and Evolution* **66:** 694–714.

Núñez H, Veloso A, Espejo P, Veloso C, Cortés A, Araya S. 2010. Nuevas especies de *Phymaturus* (grupo *palluma*) para la zona Cordillerana Central de Chile (Reptilia, Sauria, Liolaemidae). *Boletín del Museo Nacional de Historia Natural de Chile* **59:** 41–74.

Palumbi SR. 1996. Nucleic acids I: the polymerase chain reaction. In: Hillis DM, Moritz C, Mable BK, eds. *Molecular systematics*, *2nd edn*. Sunderland, Massachusetts: Sinauer, 205–247.

Pereyra EA. 1985. Nuevo iguánido del género *Phymaturus* del noroeste Argentino. *Boletín de la Asociación Herpetológica Argentina* **2:** 3–4.

Pincheira-Donoso D. 2004. Una nueva especie del género *Phymaturus* (Iguania: Tropiduridae: Liolaemini) del centro–sur de Chile. *Multequina* **13:** 57–70.

Pincheira-Donoso D, Scolaro JA, Sura P. 2008. A monographic catalogue on the systematics and phylogeny of the South American iguanian lizard family Liolaemidae (Squamata, Iguania). *Zootaxa* **1800:** 1–85.

Ramírez MJ. 2003. The spider subfamily Amaurobioidinae (Aranae, Anyphaenidae): a phylogenetic revision at the generic level. *Bulletin of the American Museum.of Natural History* **277:** 1–262.

Roig-Juñent S, Domínguez MC, Flores GE, Mattoni C. 2006. Biogeographic history of South American arid lands: a view from its arthropods using TASS analysis. *Journal of Arid Environments* **66:** 404–420.

Sabaj Pérez MH, ed. 2012. Standard symbolic codes for institutional resource collections in herpetology and ichthyology: an Online Reference. Version 3.0 (23 February 2012). Available at: http://www.asih.org/, American Society of Ichthyologists and Herpetologists, Washington, DC.

Saint KM, Austin CC, Donnellan SC, Hutchinson MN. 1998. C–mos, a nuclear marker useful for squamate phylogenetic analysis. *Molecular Phylogenetics and Evolution* **10:** 259–263.

Sambrook J, Russell DW. 2001. *Molecular cloning: a laboratory manual*, Vol. 1, *3rd edn*. New York: Cold Spring Harbor Laboratory Press.

Schulte JA, Valladares JP, Larson A. 2003. Phylogenetic relationships within iguanidae inferred using molecular and morphological data and a phylogenetic taxonomy of iguanian lizards. *Herpetologica* **59:** 399–419.

Scolaro JA. 2010. Redescripción del Neotipo de *Phymaturus palluma*: un aporte a la delimitación de su tierra típica (Reptilia, Sauria, Liolaemidae). *Boletín del Museo Nacional de Historia Natural, Chile* **59:** 29–39.

Sérsic AN, Cosacov A, Cocucci AA, Johnson LA, Pozner R, Avila J, Sites JW Jr, Morando M. 2011. Emerging phylogeographic patterns of plants and terrestrial vertebrates from Patagonia. *Biological Journal of the Linnean Society, London* **103:** 475–494.

Siddall ME. 1995. Another monophyly index: revisitng the jackknife. *Cladistics: The International Journal of the Willi Hennig Society* **11:** 33–56.

Thompson JD, Higgins DG, Gibson TJ. 1994. CLUSTAL W: improving the sensitivity of progressive multiple sequence alignment through sequence weighting, position–specific gap penalties and weight matrix choice. *Nucleic Acids Research* **22:** 4673–4680.

Troncoso-Palacios J, Esquerré D. 2014. A new species of *Phymaturus* of the *P. mallimaccii* Group from the Andes of central Chile (Iguania: Liolaemidae). *Phyllomedusa* **13:** 3–15.

Troncoso-Palacios J, Lobo F. 2012. A new species of *Phymaturus* (Iguania: Liolaemidae) of the *palluma* group from Central Chile. *Cuadernos de Herpetología* **26:** 69–78.

Troncoso-Palacios J, Lobo F, Etheridge R, Acosta JC, Laspiur A. 2013. The rediscovery of *Oplurus bibronii* Guichenot, 1848 a valid species of the liolaemid genus *Phymaturus* (Iguania: Liolaemidae). *Zootaxa* **3652:** 547–561.

Vaidya G, Lohman D, Meier R. 2011. SequenceMatrix: concatenation software for the fast assembly of multi–gene datasets with character set and codon information. *Cladistics: The International Journal of the Willi Hennig Society* **27:** 171–180.

Wassersug RJ. 1976. A procedure for differential staining of cartilage and bone in whole formalin fixed vertebrates. *Stain Technology* **51:** 131–134.

Wiens JJ. 2000. Coding morphological variation within species and higher taxa for phylogenetic analysis. In: Wiens JJ, ed. *Phylogenetic analysis of morphological data*. Washington D.C.: Smithsonian Institution Press, 115–145.

Wiens JJ, Reeder TW, Montes de Oca AN. 1999. Molecular phylogenetics and evolution of sexual dichromatism among populations of the Yarrow's Spiny lizard (*Sceloporus jarrovii*). *Evolution* **6:** 1884–1897.

Wiley EO, Siegel-Causey D, Brooks DR, Funk VA. 1991. The Compleat Cladist. The University of Kansas, Museum of Natural History, Special Publication N°19.

APPENDIX 1

List of all the species, voucher numbers, and GenBank accession numbers of the sequences employed in this study; new sequences obtained in this study are marked in bold. The species names are the same as those shown in the tree of Figure 7.

Clarifications: *P.* sp. 1 of Morando *et al.* (2013) is named here as *P. tromen* Lobo & Nenda, 2015; *P.* sp. 2 of Morando *et al.* (2013) is named here as *P. maulense* Núñez *et al.*, 2010; *P.* sp. 8 of Lobo *et al.* (2012a) is named here as *P. williamsi* Lobo, Laspiur & Acosta, 2013; *P.* cf. *palluma* of Morando *et al.* (2013) is named here as *P.* sp ups. *Asterisks mark species with gene fragments belonging to different vouchers specimens.

Species	Vouchers	12S	cytb	ND4	Cmos	NTF3	PLRL	PNN	Phy38	Phy41	Phy60	Phy64	Phy84	Phy89
P. aguedae	SSUC-Re 588	**KT203835**	**KT203826**	**KT203845**	**KT203818**	–	–	–	–	–	–	–	–	–
P. antofagastensis	MACN 44599	**KT203842**	**KT203828**	**KT203859**	**KT203824**	–	–	–	–	–	–	–	–	–
P. bibronii	SSUC-Re 0429	**KT203840**	**KT203829**	**KT203857**	**KT203822**	–	–	–	–	–	–	–	–	–
P. damasense	MNHN 4782	**KT203843**	**KT203830**	**KT203861**	**KT203825**	–	–	–	–	–	–	–	–	–
P. denotatus	MCN 3160	**KT203838**	**KT203833**	**KT203853**	**KT203820**	–	–	–	–	–	–	–	–	–
*P. dorsimaculatus**	LJAMM–CNP 983/MCN 3733	JF272814	JF272781	**KT203856**	JX969518	JX969596	JX969498	JX969421	JX969124	JX969316	JX969172	JX969111	JX969217	JX969268
*P. extrilidus**	LJAMM–CNP 538/MCN 2665	JX969070	JX969019	**KT203851**	JX969527	JX969605	JX969507	–	JX969133	JX969325	JX969180		JX969226	JX969277
P. indistinctus	LJAMM–CNP 2124	JX969084	JX969033	–	JX969538	JX969568	JX969470	JX969441	JX969147	JX969339	JX969189	JX969369	JX969240	JX969290
*P. laurenti**	LJAMM–CNP 5857/LJAMM–CNP 983/MCN 3133	JX969060	JX969009	**KT203848**	JX969517	JX969595	JX969497	JX969420	JX969123	JX969315	JX969171	JX969111	JX969216	JX969267
*P. mallimaccii**	LJAMM–CNP 2035/MCN 1741	JX969062	JX969011	**KT203847**	JX969519	JX969597	JX969499	JX969422	JX969125	JX969317	JX969173	JX969112	JX969218	JX969269
P. maulense	LJAMM–CNP 3442	JX969071	JX969020	–	–	JX969606	JX969508	JX969428	JX969134	JX969326	JX969181	JX969119	JX969227	JX969278
P. paihuanense	SSUC-Re 0426	**KT203841**	**KT203832**	**KT203858**	**KT203823**	–	–	–	–	–	–	–	–	–
P. palluma	MCN 3627	**KT203839**	**KT203834**	**KT203854**	**KT203821**	–	–	–	–	–	–	–	–	–
P. patagonicus	LJAMM–CNP 3205	JX969087	JX969036	–	JX969541	JX969571	JX969473	JX969444	JX969149	JX969341	JX969192	–	JX969243	JX969293
P. punae	LJAMM–CNP 2699	JX969064	JX969013	–	JX969521	JX969599	JX969501	–	JX969127	JX969319	JX969175	JX969114	JX969220	JX969271
*P. querque**	LJAMM–CNP 8060/MCN 3857	JX969069	JX969018	**KT203863**	JX969526	JX969604	JX969506	JX969427	JX969132	JX969324	JX969179	JX969118	JX969225	JX969276
*P. roigorum**	LJAMM–CNP 4434/MCN 2113	JX969065	JX969014	**KT203849**	JX969522	JX969600	JX969502	–	JX969128	JX969320	–	JX969115	JX969221	JX969272
*P. somuncurensis**	LJAMM–CNP 4453/MCN 4550	JX969089	JX969038	**KT203860**	JX969543	JX969573	JX969475	JX969446	JX969151	JX969343	JX969194	JX969373	JX969245	JX969295
P. sp. 3	LJAMM–CNP 5390	JX969072	JX969021	–	–	JX969607	JX969509	JX969429	JX969135	JX969327	–	JX969120	JX969228	JX969279
P. sp. 4	LJAMM–CNP 5314	JX969073	JX969022	–	JX969528	JX969608	JX969510	JX969430	JX969136	JX969328	JX969182	–	JX969229	JX969280
P. sp. 5	LJAMM–CNP 5285	JX969074	JX969023	–	–	JX969609	JX969511	JX969431	JX969137	JX969329	–	–	JX969230	JX969281
P. sp. 6	LJAMM–CNP 5260	JX969075	JX969024	–	JX969529	JX969610	JX969512	JX969432	JX969138	JX969330	JX969183	–	JX969231	JX969282
P. sp. 7	LJAMM–CNP 10560	JX969076	JX969025	–	JX969530	JX969612	JX969513	JX969433	JX969139	JX969331	–	JX969121	JX969232	JX969283
P. sp. 8	LJAMM–CNP 6175	JX969077	JX969026	–	JX969531	JX969613	JX969514	JX969434	JX969140	JX969332	JX969184	–	JX969233	JX969284
P. sp. 9	LJAMM–CNP 5222	JX969078	JX969027	–	JX969532	JX969613	JX969515	JX969435	JX969141	JX969333	JX969185	–	JX969234	JX969285
P. sp. 10	LJAMM–CNP 7900	JX969079	JX969028	–	JX969533	JX969614	JX969516	JX969436	JX969142	JX969334	–	JX969122	JX969235	–
P. sp. fia	MCN 2123	**KT203836**	**KT203831**	**KT203850**	**KT203819**	–	–	–	–	–	–	–	–	–
P. sp. gua	MCN 1642	**KT203844**	–	**KT203846**	–	–	–	–	–	–	–	–	–	–
P. sp. usp*	LJAMM–CNP 2800/MCN 2660	JX969063	JX969012	**KT203862**	JX969520	JX969598	JX969500	JX969423	JX969126	JX969318	JX969174	JX969113	JX969219	JX969270
*P. tromen**	LJAMM–CNP 5190/MCN 3713	JX969068	JX969017	**KT203855**	JX969525	JX969603	JX969505	JX969426	JX969131	JX969323	JX969178	–	JX969224	JX969275
P. verdugo	LJAMM–CNP 5793	JX969066	JX969015	–	JX969523	JX969601	JX969503	JX969424	JX969129	JX969321	JX969176	JX969116	JX969222	JX969273
P. vociferator	LJAMM–CNP 3432	JX969067	JX969016	–	JX969524	JX969602	JX969504	JX969425	JX969130	JX969322	JX969177	JX969117	JX969223	JX969274
P. williamsi	MCN 2812	**KT203837**	**KT203827**	**KT203852**	–	–	–	–	–	–	–	–	–	–

APPENDIX 2

NEW MORPHOLOGICAL CHARACTERS FOR THE GENUS *PHYMATURUS*

Below we present the list of new morphological characters that are added to the morphological data matrix of Lobo *et al*. (2012a). Several of these characters were discovered at the time of the 2012 analysis, but they were not included because they lacked a wide revision across taxa. *Asterisks refer to characters that are informative for the *palluma* group only.

**Character 208:* White scales spread out over dorsum and flanks (binary polimorphic): 0, absent; 1, present. Character shared by *P. punae*, *P.* sp. lar, *P*. sp. gua. Not fixed in any species.

Character 209: Occurrence of melanistic individuals (binary polimorphic): 0, absence; 1, presence. Character shared by *P. ceii*, *P*. cf. *ceii*, and *P. tenebrosus*. Not fixed in any species.

***Character 210:* White spots on dorsum of trunk arrangement (binary polimorphic): 0, irregularly distributed; 1, forming transversal rows (*P*. cf. *ceii*, *P. felixi*, and a few individuals of *P. calcogaster* and *P. manuelae*). Not fixed in any species.

Character 211: Tails spotted white in a similar way to dorsum of trunk: 0, absent; 1, present. Character shared by *P. delheyi*, *P. nevadoi*, *P. payuniae*, and *P. sitesi*.

Character 212: Light brown over dorsum of trunk: 0, absent; 1, present. Character shared by *P. sitesi*, *P. tenebrosus*, and *P. zapalensis*.

**Character 213:* Dorsal mesenterium of large intestine pigmentation (Fig. 6A and B): 0, absent (translucid); 1, present (melanic pigmented).

**Character 214:* External wall of rectum (multistate polymorphic; Fig. 6C): 0, smooth; 1, shallowly striated; 2, deeply striated.

**Character 215:* Internal mucosa of rectum (Fig. 6D): 0, simple, without folds; 1, small longitudinal folds; 2, large longitudinal folds.

**Character 216:* Pigmentation of connective dorsal fascia of axial musculature (Fig. 7): 0, no pigmentation; 1, dorsal fascia of transversospinalis pigmented; 2, dorsal fascia of both epiaxial muscles pigmented (light brown); 3, dorsal fascia of longissimus dorsi brown

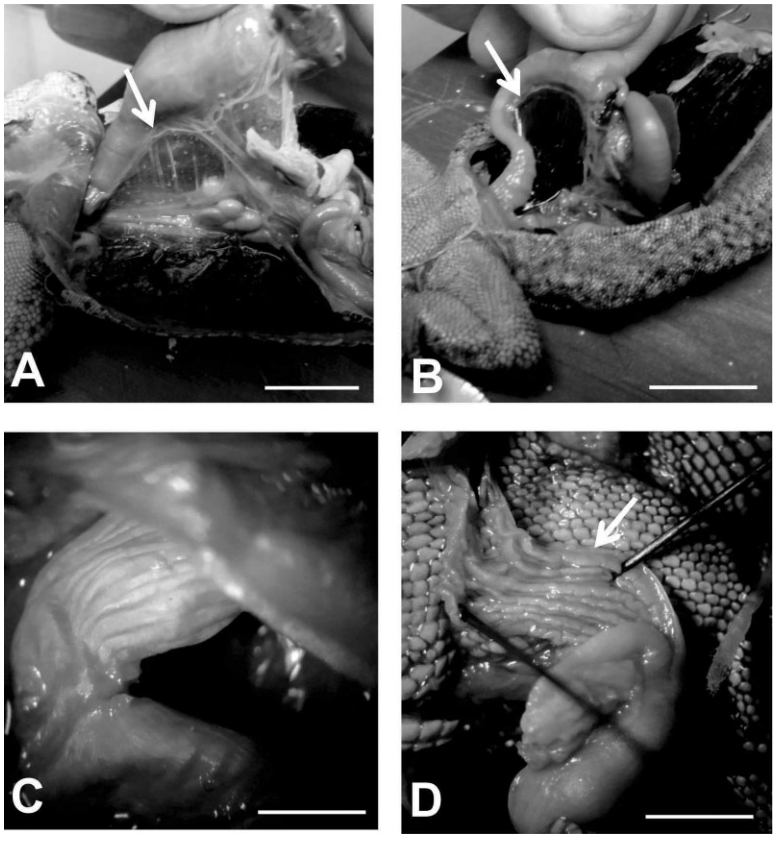

Figure 6. A, transparent mesenterium of *Phymaturus palluma* (MCN 2651; character 213). Scale bar: 10 mm. B, same mesenterium, but completely melanic in *Phymaturus patagonicus* (MCN 3561). Scale bar: 10 mm. C, external surface of rectum of *Phymaturus verdugo* (MCN 1961; character 214). Scale bar: 5 mm. D, Longitudinal folds of the internal mucosa of rectum in *Phymaturus payuniae* (MCN 2879; character 215). Scale bar: 5 mm.

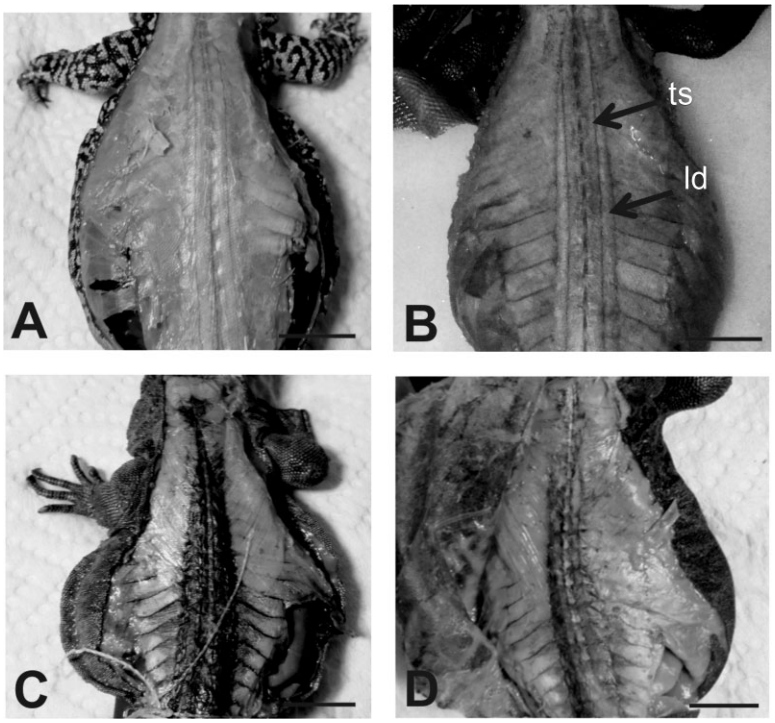

Figure 7. Epiaxial musculature fascia (characters 216–219): A, no pigmentation of fascia dorsal among axial muscles of *Phymaturus roigorum* (MCN 2102); B, lateral pigmentation between axial muscles forming longitudinal lines, neural spines delineated in black in *Phymaturus aguanegra* (MCN 3288). C, lateral and dorsal fascia of axial muscles pigmented in *Phymaturus spurcus* (FML 1244). D, same condition, but less melanic, observed in *Phymaturus tenebrosus* (MCN 1263). Neural spines highlighted in white. Scale bars: 10 mm. Abbreviations: ld, longissimus dorsi muscle; ts, transversospinalis muscle.

pigmented and transversospinalis without pigmentation; 4, dorsal fascia dark brown, but lateral fascia still evident; 5, dorsal fascia dark brown, lateral fascia difficult to recognize.

**Character 217:* Anterior projection of dorsal fascia melanism: 0, only reaching level of shoulders; 1, reaching level over nuchal musculature.

**Character 218:* Neural spines (Fig. 7B and D): 0 , neural spines inconspicuous; 1, neural spines of vertebrae notable from the transversospinalis pigmentation.

**Character 219:* Number of pigmented longitudinal/lateral fascia separating epaxial muscles (Fig. 7): 0, absent; 1, five; 2, six; 3, seven; 4, eight; 5, nine.

**Character 220:* Dorsal tibial scale shape (binary polymorphic; Fig. 8): 0, round (juxtaposed); 1, subpentagonal elongated in the proximal–distal axis (subimbricated).

**Character 221:* Relative size of dorsal and anterior tibial scales (binary polymorphic): 0, similar size; 1, dorsal tibial scales larger than anterior scales.

**Character 222:* Tibial scale structures (Fig. 8B): 0, dorsal tibial scales with spines and scale organs on their distal tips; 1, dorsal tibial scales with scale organs (not spines).

**Character 223:* Granular scales among dorsal tibials (Fig. 8F): 0, absent; 1, present (binary polymorphic).

**Character 224:* Posterior tibial scales (binary polymorphic): 0, enlarged in the distal third of tibia length; 1, enlarged along its entire length.

**Character 225:* Pigal scales of the posterior half of the precloacal region: 0, smaller in females than in males; 1, similar size in both sexes.

**Character 226:* Fecundity (species average number of embryos per female): 0, 1.00; 1, 1.5–1.66; 2, 1.75–1.77; 3, 1.80; 4, 2.00–2.25; 5, 2.66; 6, 3.0. This character would be analysed as a continuous character, but sample sizes are limited, and because *Phymaturus* species are considered 'vulnerable' in Abdala *et al*. (2012), collecting pregnant females to achieve more accurate information is not recommended. Most species exhibit states 2–4.

Character 227: Ocelli formed by the incomplete and irregular confluence of white spots: 0, absence; 1, presence.

Character 228: Females with bright yellow over cloaca and thighs and posterior region of abdomen orange: 0, absent; 1, present (*P. tenebrosus* and *P. zapalensis*).

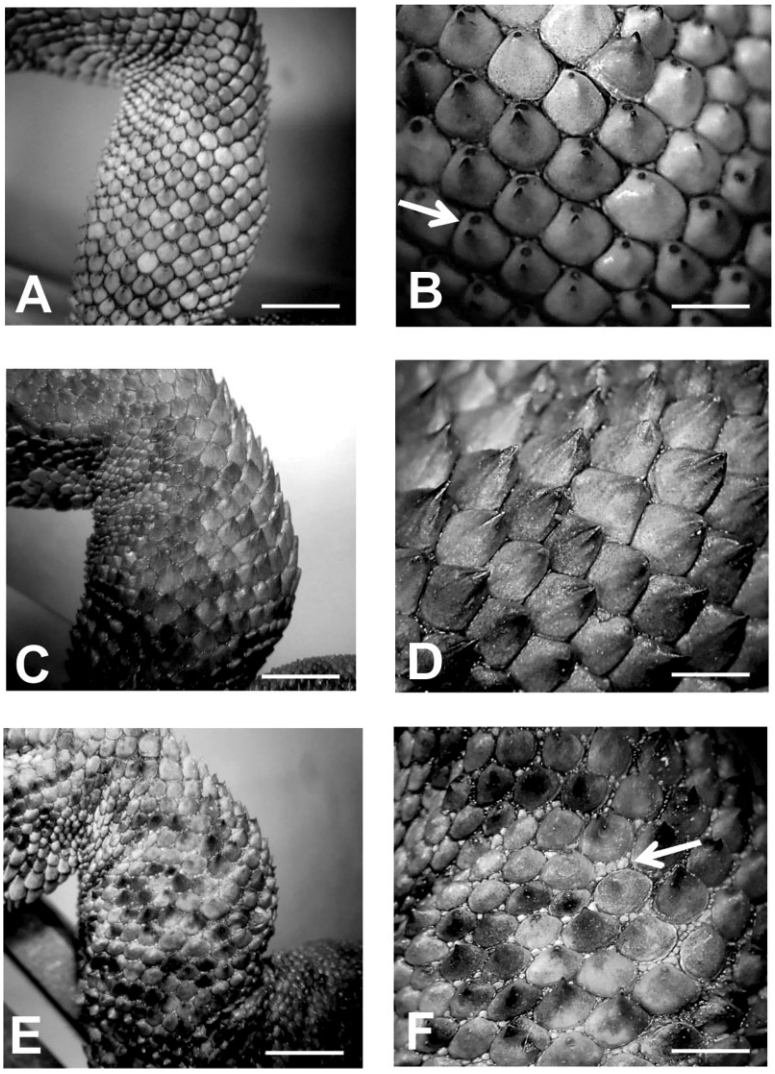

Figure 8. A, tibial dorsal scalation of *Phymaturus patagonicus* (MCN 3561). B, central area of the same view of *P. patagonicus* (same specimen) tibia, showing scales in detail (character 220). Almost every dorsal tibial scale carries a spine and a scale organ on the distal tip of the scale (arrow; character 222). C, tibial dorsal scalation of *Phymaturus palluma* (MCN 3131). D, central area of the same view of *P. palluma* (same specimen). Scale organs hidden under the scale spines. E, tibial dorsal scalation of *Phymaturus denotatus* (MCN 3160). F, central area of the same view of *P. denotatus* (same specimen). The arrow indicates granular scales spread out among tibial scales (character 223). Scale bars: A, C, E, 5 mm; B, D, F, 2 mm.

Character 229: Ontogenetic sequence of transversal row of white spots (step matrix/Sankoff).

Character 230: Ontogenetic sequence of black transversal stripes (step matrix/Sankoff).

Character 231: Ontogenetic sequence of light-brown ocelli (step matrix/Sankoff).

Character 232: First chevron location: 0, beyond second caudal vertebra; 1, second caudal vertebra.

**Character 233:* Number of temporal scales with two or more scale organs/number of temporal scales with only one scale organ (Fig. 9A): 0, <0.20; 1, ≥0.20.

**Character 234:* Nasal salt excretion: 0, absent; 1, present (Lobo *et al*., 2012c: fig. 5). At this time found only in the Puna clade: *P. aguedae*, *P. bibronii*, *P. denotatus*, *P. extrilidus*, *P. laurenti*, *P. paihuanense*, and *P.* sp. lar.

**Character 235:* Scale organs on rostral scale (binary polymorphic): 0, present; 1, absent.

**Character 236:* Number or scales between the row of precloacal pores and the anterior border of cloaca (Fig. 9B): 0, 0–4 scales; 1, ≥5 scales. The plesiomorphic condition is exhibited by *Ctenoblepharys* and *Liolaemus* (state 0), see Etheridge (1995).

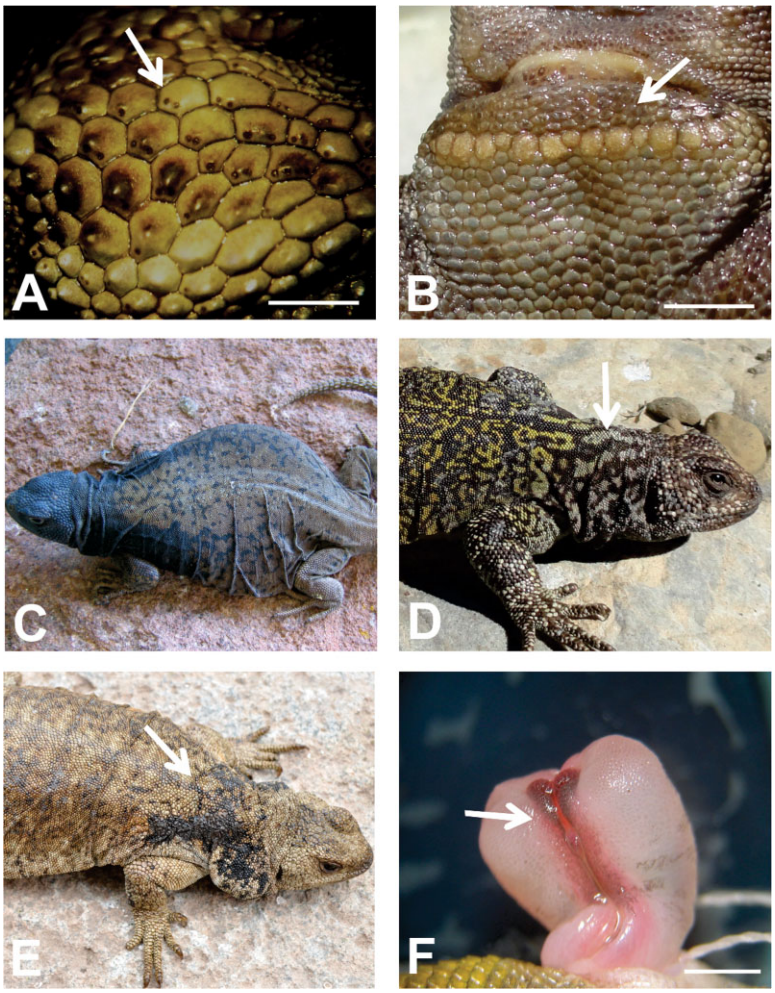

Figure 9. A, temporal scales of *Phymaturus dorsimaculatus* (MCN 1569) showing two organ scales (character 233); scale bar, 2 mm. B, cloacal region of *Phymaturus verdugo* (MCN 1960; Character 236); scale bar, 5 mm. C, female of *Phymaturus verdugo* (MCN 1958; snout–vent length, SVL = 99.8 mm; character 237). D, *Phymaturus querque* male (MCN 3863; SVL = 104.9 mm; character 249). E, *Phymaturus paihuanense* female (SSUC–Re 0422; photo by A. Laspiur; character 252). F, hemipenis of *Phymaturus roigorum* (MCN 1963; character 253); scale bar, 5 mm.

**Character 237:* Part of adult female population with the whole body brown 'chocolate' coloration (binary polymorphic; Fig. 9C): 0, absence; 1, presence. Character shared by *P. dorsimaculatus*, *P. tromen*; *P. verdugo*.

**Character 238:* Supratemporal shape: 0, wide, with its lower margin convex, resembling the shape of a knife; 1, slender, upper and lower margins straight and parallel.

**Character 239:* Supratemporal length: 0, long, its anterior tip reaches at least a position at the level of the posterior medial margin of parietal, close to the epipterygoid connection; 1, short, not reaching this level, just half of the squamosal process of the parietal.

**Character 240:* Orbitosphenoid ossification (Figs 10A and B): 0, reaching dorsally the ventral margin of fenestra epioptica; 1, not reaching this fenestra.

**Character 241:* Posteromedial process of ectopterygoid (multistate polymorphic; Figs 10C and D): 0, absent; 1, round and short; 2, forming a curved spine with a cartilage at its free ending.

**Character 242:* Lateral and lateral–dorsal antebrachial scales: 0, round and smooth; 1, round to leaf-shaped, with a posterior small spine; 2, leaf-shaped, with a conspicuous posterior spine.

**Character 243:* Enlarged external postcloacal scales in males: 0, absent; 1, present.

**Character 244:* Scale organs under spines of dorsal and lateral tail scales: 0, absent; 1, one or two scale organs. Present in *P.* sp. lar, absent in *P. dorsimaculatus*.

Character 245: Mid-dorsal longitudinal band formed by enlarged white spots irregularly distributed (binary polymorphic): 0, absence; 1, presence.

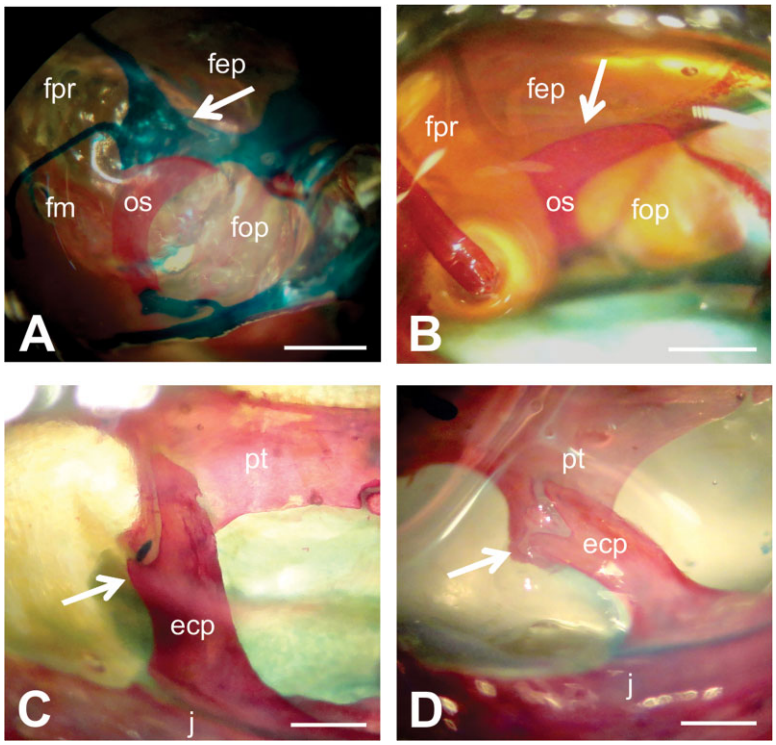

Figure 10. A, orbitosphenoid bone in *Phymaturus aguanegra* (MCN 968; character 240); the arrow indicates the cartilaginous margin of the fenestra epioptica. B, *Phymaturus zapalensis* (MCN 1486). C, ectopterygoid of *Phymaturus spurcus* (MCN 1249; character 241). D, same bone in *Phymaturus laurenti* (MCN 326). Abbreviations: ecp, ectopteygoid; fep, fenestra epioptica; fm, fenestra metoptica; fop, fenestra optica; fpr, fenestra prootica; j, jugal; pt, pterygoid. Scale bars: 1 mm.

**Character 246:* Fusion of first postocular with subocular scale (binary polymorphic): 0, absent; 1, present. Not fixed in any species. Significant variation within the *patagonicus* group; only detected in *P.* sp. gua within the *palluma* group.

**Character 247:* Wide opening of nares with its anterior lower border projected inside the opening, forming a flat and wide surface (binary polymorphic): 0, absent; 1, present. Not fixed in any species.

**Character 248:* Irregularly divided row of precloacal pores (not at the middle; binary polymorphic): 0, absent; 1, present. Not fixed in any species.

**Character 249:* Males with yellow dorsum becoming white on the neck (binary polymorphic): 0, absent; 1, present (Fig. 9D). Not fixed in any species.

**Character 250:* Dorsal and lateral tail scales with longitudinal rugosities: 0, absent; 1, present (*palluma* group apomorphy). Not listed in Lobo & Quinteros (2005), but described in the discussion under the section 'Observations on the ontogenetic shift of morphological characters'. In advanced unborn fetuses and juveniles of the *palluma* groups these scales are smooth (as in juvenile and adult individuals of the *patagonicus* group), becoming rugose later.

**Character 251:* Juvenile pattern provided of paravertebral irregular shaped markings: 0, absence; 1, presence.

**Character 252:* Melanic spots on sides of neck and shoulders (binary polymorphic): 0, absence; 1, presence (Fig. 9E). Not fixed in any species.

**Character 253:* Hemipenis pigmentation: 0, sulcus melanic, with pigmentation invading surface of lobes; 1, sulcus completely melanic, with pigmentation projected in both branches of its bifurcation, lobes immaculate (Fig. 9F); 2, completely unpigmented.

APPENDIX 3

A total of 563 *Phymaturus* specimens were examined for morphological study, representing 21 recognized species and seven other unnamed taxa. Institutional abbreviations follow Sabaj Pérez (2012), with the following additions: MCN, Museo de Ciencias Naturales, Universidad Nacional de Salta, Salta, Argentina; REE–CSUN, Robert E. Espinoza, California State University, Northridge, California, USA; REE–SDSU, Richard E. Etheridge skeletal collection, San Diego State University, San Diego, California, USA; and SSUC–Re, Colección de Flora y Fauna, Profesor Patricio

Sánchez Reyes de la Pontificia Universidad Católica de Chile. Skeletonized specimens are indicated by CS (cleared and stained skeletons) and DS (dry skeletons).

Phymaturus aguanegra (*N* = 30; sp. 9 in Lobo *et al*., 2012a): MCN 975 (holotype, male) Paso Agua Negra (30°23′S, 69°34′W, 2900 m. a.s.l.), Iglesia Department, San Juan Province, Argentina. *Paratypes:* MCN 969, 973–975, 977, 979, 982, 984, 988, 990–991, 995 and 971–972, 976, 978, 980, 981, 983, 986–987, 989, 992–993. MCN 984–5 (CS). Same data as holotype.

Phymaturus aguedae (*N* = 7): SSUC–Re 588 (holotype, male) near the summit of the Provincia.

Mountain (33°25′S, 70°26′W, 2712 m. a.s.l.), Metropolitan Region, Chile.

Paratypes: SSUC–Re 592, near the summit of Provincia Mountain in the 'Paso de Piedras', 2707 m a.s.l.

SSUC–Re 595–96, SSUC–Re 593–94, near the summit of Provincia Mountain, between 2683 and 2716 m a.s.l. SSUC–Re 589, near the summit of the Provincia Mountain, 2707 m a.s.l.

Phymaturus antofagastensis (*N* = 15): MCN 309–10, road to Paso San Francisco, Antofagasta Department, Catamarca Province, Argentina. MCN 1429–36, 130 km from Fiambalá on the road to Paso San Francisco; Antofagasta Department, Catamarca Province, Argentina. SDSU 1991, Agua de los Pocitos, Antofagasta Department, Catamarca Province, Argentina. FML 2019–10 and FML 2019–13 (CS) destacamento Las Grutas – 20 km east of Paso San Francisco, 4100 m a.s.l., Tinogasta Departament, Catamarca Province, Argentina. FML 1861–5, M1861–11 (CS) Las Grutas, 4200 m a.s.l., Gendarmería Station, 20 km east of Paso San Francisco, Tinogasta Departament, Catamarca Province, Argentina.

Phymaturus bibronii (*N* = 5): SSUC–Re 0428–32 Andean highlands of Ovalle, 33 km east of Los Molles, near Los Patos pass (30°43′58″S, 70°19′56″W, 3176 m a.s.l.), Chile.

Phymaturus paihuanense (= *P. bibronii*; *N* = 12): MNHN–CL 4051–54 Los Piuquenes Valley, Paihuano, Río Claro, (30°23′S, 70°23′W, 3194 m a.s.l.). SSUC–Re 0412, 0421–27 Quebrada Los Piuquenes, Alcohuaz, Paihuano, Río Claro, Coquimbo region, Chile.

Phymaturus damasense (*N* = 10): MNHN–CL 4782 Las Damas river, approximately 1.5 km east of Termas del Flaco (34°57′56″S, 70°24′45″W), 66 km south-east of San Fernando, Región del Libertador Bernardo O'Higgins, Chile. MNHN–CL 4745–48. Termas del Flaco, Región del Libertador Bernardo O'Higgins, Chile. SSUC–Re 0413–17. Las Damas river, aproximately 1.5 km east of Termas del Flaco (34°57′56″S, 70°24′45″W), 66 km south-east of San Fernando, Región del Libertador Bernardo O'Higgins, Chile.

Phymaturus dorsimaculatus (*N* = 25): MCN 1573 (holotype); MCN 1571–72, 1574–75 (paratypes); MCN 1566–67 and 1487–88 (CS), Copahue (37°49′S, 71°06′W), Ñorquin Department, Neuquén Province, Argentina. MCN 1568–69, Termas de Copahue (37°49′14′S, 71°05′12′W, 2050 m a.s.l.), Ñorquin Department, Neuquén Province, Argentina. MVZ 232503, Termas de Copahue (2050 m a.s.l.), Ñorquin Department, Neuquén Province, Argentina. MCN 3727–3732 on the road between El Huecu and Colipilli (37°44′06.6″S, 70°28′52.1″W, 1545 m a.s.l.), Ñorquin Department, Neuquén Province, Argentina. MCN 3733–40, 3779. North from Huecu (37° 36′31.1″S, 70°37′53.5″W, 1638 m a.s.l.), Ñorquin Department, Neuquén Province, Argentina.

Phymaturus denotatus (*N* = 21): MACN 40512 (holotype) and MACN 40513–17, MCN 3159, MCN 3160–61, 3170, 3176–79, 3181, 3183, 3186–89 (paratypes). Laguna Blanca, (26°34′09′S, 66°56′40′W, 3440 m a.s.l.). Belén Department, Catamarca Province, Argentina.

Phymaturus extrilidus (*N* = 37): MCN 2657, MCN 2655–56, 2665–66, 2669–71, 2673, 2721–35, 2737, Don Carmelo, along hillside (Sierra La Invernada) behind field station (30°55′91′S, 69°04′98′W, 3133 m a.s.l.), Ullum Department, San Juan Province, Argentina. MCN 2709–20 (paratypes), Reserva Natural de Uso Múltiple Don Carmelo, Aguada de Pinchagua (30°58′66′S, 69°05′21′W, 3122 m a.s.l.), Ullum Department, San Juan Province, Argentina.

Phymaturus indistinctus (*N* = 24): IBA 666-1 (holotype), IBA 666-2–3, Lago Munsters, 2 km west of Las Pulgas, 700–800 m a.s.l., Sarmiento Department, Chubut Province, Argentina. MCN 1274–77, Las Pulgas, hill opposite the Virgin Grotto, Sarmiento Dept, Chubut Province, Argentina. MCN 3943–55, 19 km west of Los Manatiales, Provincial Route 20, 45°27′S; 69°42′W, 669 m a.s.l., Sarmiento Dept., Chubut Province, Argentina.

Phymaturus laurenti (*N* = 44): MCN 2855 (holotype), MCN 2838–54, 2856–62 (paratypes), 10 km south of El Peñón on rocky outcrops 300 m east of Provincial Road 43 (26°39′40.6′S, 67°13′26.3′W, 3815 m a.s.l.), Antofagasta Department, Catamarca Province, Argentina. MCN 306–07, 323–27, Cuesta de Calalaste; Antofagasta Department, Catamarca Province, Argentina. MCN 313–17, 320, 322, Cuesta de Randolfo; Antofagasta Department, Catamarca Province, Argentina. MCN 1919–21, north Antofagasta de la Sierra (25°38′06″S, 67°13′53.65″W), Antofagasta Department, Catamarca Province, Argentina. MCN 3133, east of El Peñón, road to Cerro Galán, Antofagasta de la Sierra (26°20′28.88′S, 67°08′1.51′W), Antofagasta Department, Catamarca Province, Argentina.

Phymaturus mallimaccii (*N* = 5): MCN 920 on the road to La Mejicana (28°54′43′S, 67°42′47′W, 3430 m a.s.l.), Sierra de Famatina, Famatina Depart-

ment, La Rioja Province, Argentina. REE–CSUN 183, 489–491, Sierra de Famatina, Cueva de Pérez, Famatina Department, La Rioja Province, Argentina. MCN 1741, Cueva de Pérez, Famatina Department, La Rioja Province, Argentina.

Phymaturus maulense (*N* = 16): MNHN–CL 3938–42, 3945, 4038–39 Vilches Alto (35°35′S, 70°58′W, 2189 m a.s.l.), El Enladrillado, Reserva Nacional Altos de Lircay, Región del Maule, Chile. MZUC 35959–60, Enladrillado, Lircay, Talca Province, Región del Maule, Chile. MVZ 232506–07, on road to Laguna del Maule (Los Cóndores pass), Talca Province, 1800 m a.s.l., Región VII (= Región del Maule), Chile (R. Sage coll.). SSUC–Re 0410–11, Laguna del Maule, Talca Province, Región VII, Chile. MNHN–CL 2353, 2460–61. Baños del Campanario (1500 m a.s.l.), Talca, San Clemente, Chile.

Phymaturus palluma (= *Phymaturus gynechlomus*; *N* = 32). MCN 3130–3131, Portillo Argentino (Cordón del Portillo, 33°36′53.8″S, 69°29′16.7″W), Mendoza Province, Argentina. MCN 3612–13, 3619–22, Portillo Argentino, Arroyo Guardia Vieja (33°36′53.8″S, 69°29′16.7″W), Mendoza Province, Argentina. MVZ 126991, Valle Hermoso (35°20′S, 70°15′W), Malargüe Departament, Mendoza Province, Argentina. MVZ 126992–126894, Lago de la Niña Encantada (33°18′S, 69°83′W, 2000 m a.s.l.), 6 km east of Molles, Mendoza Province, Argentina. MVZ 126995, at the north end of Valle Hermoso (35°11′S, 70°10′W), Malargüe Departament, Mendoza Province, Argentina. MVZ 126996–126999, 4 km NW from Cerro Chupasangral (33°21′S, 69°51′W, 2800 m a.s.l.), Quebrada de Chupasangral, Tupungato Department, Mendoza Province, Argentina. MVZ 127025–127027, 2 km east from Agua Botada (35°62′S, 69°95′W), Malargüe Departament, Mendoza Province, Argentina. MVZ 180771–180774, Quebrada Cruz de Piedra (34°26′S, 68°90′W), San Carlos Departament, Mendoza Province, Argentina. MCN 3627–30, 3635–43, 3645, Road to Laguna Diamante (34°14′33.6″S, 69°24′00.0″W), San Carlos Departament, Mendoza Province, Argentina.

Phymaturus patagonicus (*N* = 35): MLP 778 (lectotype), MLP 777 (paralectotype), Argentina, Territorio del Chubut, Patagonia. FML 10077–85, 1 km west of intersection between Provincial Routes 53 and 90, 2.2 km south-west of Meseta El Sombrero Paso de Los Indios Department, Chubut Province, Argentina. IADIZA 80, 40 km west Dolavon, 350 m a.s.l., Gaiman Department, Chubut Province, Argentina. IBA 783, 5, 20 km west of Sombrero; Paso de Los Indios Department, Chubut Province, Argentina. IBA 789, 7, MCN 1284–86, 40 km west of Dolavon, Gaiman Department, Chubut Province, Argentina. MCN 1250–58, 1261, Paso de Los Indios Department, hills in front of El Sombrero, Chubut Province, Argentina. SDSU 1980, 40 km west of Dolavon, Gaiman Department, Chubut Province, Argentina.

Phymaturus punae (*N* = 21): MCZ 19217 (holotype), MCZ 163982, 163984, 163986–88 (paratypes), Río San Guillermo (3500 m a.s.l.), 7 km south-east of refuge in Provincial Reserve, Iglesia Department, San Juan Province, Argentina. MCN 3114–26, Reserva Provincial San Guillermo, Iglesia Department, San Juan Province, Argentina. SDSU 1978–79, Reserva Provincial San Guillermo, Llano de los Hoyos, Iglesia Department, San Juan Province, Argentina.

Phymaturus querque (*N* = 24): FML 21556 (holotype), FML 21211, IBA 793 (paratypes), Laguna Blanca, Laguna Blanca National Park, Zapala Department, Neuquén Province, Argentina. MACN 34514 (five individuals) Laguna Blanca, Zapala Department, Neuquén Province, Argentina. MVZ 232504–05 Puesto Control, 3.5 km north of Cerro de la Laguna, Laguna Blanca National Park, Zapala Department, Neuquén Province, Argentina. SDSU 1971, south shore of Laguna Blanca, Zapala Department, Neuquén Province, Argentina. MCN 3854–66, 9.5 km south from Laguna Blanca, Road 46 (39°08′02.40′S, 70°25′45.80′W, 1387 m a.s.l.), Zapala Department, Neuquén Province, Argentina.

Phymaturus roigorum (*N* = 31): MCN 1963 (holotype), FML 17705–08 (paratypes), and MCN 1962 Puesto Rojas, 16 km from Road Provincial 180, El Nevado, San Rafael Department, Mendoza Province, Argentina. MCN 2096–103 (paratypes), 6 km south of Real del Molle, on base of Volcán Payún Liso (36°28′51.1′S, 69°22′27.9′W, 2128 m a.s.l.) Malargüe Department, Mendoza Province, Argentina. MCN 2113–15 Real del Molle, Malargüe Department, Mendoza Province, Argentina. IADIZA 91 Base of Volcán Payún (1800–2000 m a.s.l.), Malargüe Department, Mendoza Province, Argentina. IBA 733 (five specimens) Base Camp, south-west side of Volcán Payún, Malargüe Department, Mendoza Province, Argentina. SDSU 1948–51, 1956, 1962, 1964–65 km north-west of base of Volcán Payún, Malargüe Department, Mendoza Province, Argentina. SDSU 1972, 1974–75 10 km south of base of Volcán Payún, Malargüe Department, Mendoza Province, Argentina.

Phymaturus tromen (*N* = 8). MCN 3719 (holotype; male) Road Provincial 37, route from Chos Malal to Tromen, before reaching Tromen (37°10′38.5″S, 70°10′16.2″W), Chos Malal Departament, Neuquén Province, Argentina. Paratypes: MCN 3720 (male), MACN 45430 (ex MCN 3713, female), MCN 3714 (female), MCN 3717–18 (females), MACN 45431 (ex MCN 3715, juvenile female), MCN 3716 (juvenile female), same data as holotype.

Phymaturus williamsi (*N* = 18) (sp. 8 in Lobo *et al*., 2012a). MCN 2820 (holotype, male) 40 km west of Calingasta town (31°11′21″S, 69°42′15.1″W, 3000 m a.s.l.),

Quebrada Vallecito, Calingasta Department, San Juan Province, Argentina. Paratypes: MCN 2808–10, 2812–14, 2815, 2816–17, 2821 same data as holotype. MCN 3259–65 (topotypes) same data as holotype.

Phymaturus somuncurensis ($N = 29$): IBA 470, 2, type series, MACN 37436–40, MCZ 156909, 170443–44, Laguna Raimunda, Meseta de Somuncurá, 9 de Julio Department, Río Negro Province, Argentina. FML 1038, Laguna Raimunda, Meseta de Somuncurá, 1400 m a.s.l., Valcheta Department, Río Negro Province, Argentina. IADIZA 212, Meseta de Somuncurá, Cerro Corona, 9 de Julio Department, Río Negro Province, Argentina. IBA 507, 4, Argentina, Río Negro Province, 9 de Julio Department, near Laguna Raimunda, Meseta de Somuncurá. MACN 37431–35, 2 km north of Casco Cecchi, Meseta de Somuncurá, 9 de Julio Department, Río Negro Province, Argentina. REE–SDSU 2433–35, north of Laguna Raimunda, Meseta de Somuncurá, Valcheta Department, Río Negro Province, Argentina. SDSU 1780–83, 2 km north of Laguna Raimunda, Meseta Somuncurá, 9 de Julio Department, Río Negro Province, Argentina. MCN 4550 (SJ 25), 41°12′13.95″S, 66°53′31.94″W, 1060 m a.s.l., Meseta Somuncurá, 9 de Julio Department, Río Negro Province, Argentina.

Unnamed terminal taxa

Phymaturus sp. usp (Uspallata species; $N = 63$). SDSU 1969–1970, 20 km north-east of Uspallata, 2500 m a.s.l., Las Heras Department, Mendoza Province, Argentina. SDSU 3387, 27 km north-east of Uspallata (32°28′52.2″S, 69°09′59.2″W, 2768 m a.s.l.), La Heras Department, Mendoza Province, Argentina. SDSU 3388 27 km north-east Uspallata (32°28′52.2″S, 69°09′59.2″W, 2768 m a.s.l.), La Heras Department, Mendoza Province, Argentina. MVZ 145146, Pampa de Canota (32°65′S, 69°27′W, 3000 m a.s.l.), Las Heras Department, Mendoza Province, Argentina. MVZ 92902, 92904, 92908 (DS), Las Heras Department, Mendoza Province, Argentina. REE–SDSU 2306–2307, 2312–2313, 2315 (DS), 20 km north-east of Uspallata, 2500 m a.s.l. IADIZA–CH, south and north of Paramillos (two specimens), Mendoza Province, Argentina. IBA 760 (four specimens): Paramillos, Mendoza, 2000 m a.s.l., Argentina. MCN 2650–2653, 2659–2662, 2696–2708, El Portezuelo, San Juan Province, Argentina. MCN 3614–17, 3624–26 Paramillos (32°28′59.3″S, 69°07′36.5″W), Mendoza Province, Argentina, MVZ 127023, 2 km east of Los Hornillos (32°51′S, 68°99′W), Las Heras Department, Mendoza Province, Argentina.

Phymaturus sp. gua ($N = 25$). MCN 1641–43, El Peñón (29°41′28,9″S, 68°48′39,3′W. 2820 m a.s.l.), west of Gualcamayo, San Juan Province, Argentina. MCN 3529–3544, Cerro El Overito (29°65′833″S, 68°86′104′W), San Juan Province, Argentina (3541, 3534 CS). MCN 4075–78, Puesto Los Overitos, Estancia de Abra Grande, Sierra del Overito, 15.8 km south of Escuela Albergue Provincial, Jachal Department, San Juan Province, Argentina.

Phymaturus sp. fia ($N = 3$). MCN 2122–23, 2125 Puesto la Lagunita, 35–38 km north-east of Medanitos, climbing from Medanitos to Sierra de Fiambalá, Catamarca Province, Argentina.

Phymaturus sp. chi. ($N = 7$) (= *Phymaturus* cf. *palluma* CH in Lobo & Quinteros, 2005; sp. 2 in Lobo *et al*., 2012a). MVZ 199435–38 and 230992, Hotel Termas de Chillán, Región VIII (= Región del Bío Bío), Chile. MCZ 165456 Cordillera de Chillán, Chile. MCZ 169935, Cordillera de Chillán, Chile.

Phymaturus sp. lar ($N = 61$; *Phymaturus* cf. *punae* LR in Lobo & Quinteros, 2005; sp. 6 in Lobo *et al*., 2012a). REE–CSUN 270–271, 504–508 Puesto Leoncito, Reserva Laguna Brava, Agua Quemada, La Rioja Province, Argentina. FML 2925–2, 4, 8–11,13 Puerta Quebrada del Leoncito, road to Laguna Brava, 57 km from Alto Jagüel, Sarmiento Deptartament, La Rioja Province, Argentina. FML 2926 (1–3), Agua Quemada, road to Laguna Brava, Alto Jagüel, Sarmiento Departament, La Rioja Province, Argentina. FML 2942, Quebrada del Leoncito, on the road to Laguna Brava, La Rioja Province, Argentina.

Phymaturus sp. pla ($N = 11$; *Phymaturus* cf. *palluma* EP in Lobo & Quinteros, 2005; sp. 3 in Lobo *et al*., 2012a). MNHN 2352, 2460–61, Baños del Campanario (1500 m a.s.l.), Talca, San Clemente, Chile. MNHN 3505–09, Curicó Puesto Militar San Pedro (35°10′S, 70°36′W), Pichuante, Cuesta Vergara, Chile. MNHN 1632–33, 1638, El Planchón (Int. Curicó), Chile. MNHN 1643, same data (CS).

Phymaturus sp. 10 ($N = 8$; after Morando *et al*., 2013). MCN 1958, 1960–61, Río El Gancho, 4 km from Las Loicas, Malargüe Department, Mendoza Province, Argentina. MCN 1973–77 road to El Pehuenche, 12.5 km from Las Loicas to Bardas Blancas, Malargüe Department, Mendoza Province, Argentina.